Opportunities to Improve Monitoring of Temporal Trends with FIA Panel Data

Raymond L. Czaplewski[1] and Michael T. Thompson[2]

***Abstract**: The Forest Inventory and Analysis (FIA) Program of the Forest Service, Department of Agriculture, is an annual monitoring system for the entire United States. Each year, an independent "panel" of FIA field plots is measured. To improve accuracy, FIA uses the "Moving Average" or "Temporally Indifferent" method to combine estimates from multiple panels that were measured during recent years. However, time-series estimators better serve monitoring objectives than temporally indifferent methods.*

This paper reviews the Kalman filter, which is a linear, minimum variance, sequential, model-based, time-series estimator based on the simple composite estimator. The Kalman filter combines predictions from a population dynamics model with the observed time-series of annual FIA panel estimates. This combination of design-based and model-based methods reduces serious risks from model bias, yet preserves the gain in precision from the model. Alternative models in the Kalman filter represent alternative hypotheses that may be ranked based on their relative agreement with design-based panel estimates. For example, does a model that includes the expected consequences of climate change on average rates of tree growth, regenerations and mortality better fit the annual FIA design-based panel estimates than a model that assumes no climate change?

The Kalman filter is presented in a tutorial style that relies more on graphical examples than mathematical equations. Hopefully, this genre builds awareness and confidence in this somewhat unfamiliar statistical estimator. The Kalman filter and Moving Average estimators are compared with hypothetical simulations of changing populations. A final set of examples is based on annual FIA panel estimates for the State of Colorado from 2002 to 2007, where epidemic levels of mountain pine beetle infestation are causing catastrophic tree mortality in lodgepole pine forests.

Three analysis questions are addressed. Is there an observable trend in population parameters over time? Does the trend make sense? Is the trend significant relative to the uncertainty in the population estimates?

Keywords: Forest monitoring, Kalman filter, composite estimator, *Pinus contorta*, *Dendroctonus ponderosae*, population dynamics model, AIC, information-theoretics.

1 United States Forest Service; Rocky Mountain Research Station; Inventory, Monitoring, and Analysis Program; 240 W. Prospect; Fort Collins, CO 80526 rczaplewski@fs.fed.us; http://www.fs.fed.us/rm/ogden/

2 United States Forest Service; Rocky Mountain Research Station; Inventory, Monitoring, and Analysis Program; 507 25th Street; Ogden, UT 84401; mtthompson@fs.fed.us; http://www.fs.fed.us/rm/ogden/

In: McWilliams, Will; Moisen, Gretchen; Czaplewski, Ray, comps. 2009. Forest Inventory and Analysis (FIA) Symposium 2008; October 21-23, 2008; Park City, UT. Proc. RMRS-P-56CD. Fort Collins, CO: U.S. Department of Agriculture, Forest Service, Rocky Mountain Research Station. 1 CD.

Introduction

The U.S. Forest Service Research and Development branch, through its Forest Inventory and Analysis (FIA) program, has long been committed to the delivery of current, consistent, and credible information about the status, condition, and trends of America's forests across all land ownerships and conditions. FIA has made impressive progress during the past 10 years in annual updates to these forest inventories. However, the recent FIA strategic plan for 2007-2011 (U.S. Forest Service, 2007a) stresses the importance of monitoring changes over time in forest conditions, which goes beyond an annually updated forest inventory. Monitoring changes over time is critically important to substantive strategic analyses of the nation's forests and the long-term relevance of the FIA program.

FIA has used "periodic surveys" since its inception in the 1930's. Bechtold and Patterson (2005:82) define a periodic survey as is a "*strategy whereby a set of inventory panels is measured simultaneously over a short time frame, often 1 to 3 years in the case of FIA, and there is a time lag, often many years, before the panels are remeasured.*" During recent years, FIA has re-engineered itself by moving from periodic surveys to annual surveys, in which a small sub-sample of field plots is re-measured every year in every county. Relative to periodic surveys, annual surveys are expected to improve the ability to detect and interpret changes in forest conditions (Gadbury and others 2004). McRoberts (2005) highlights the need for statistical estimators that combine population estimates or sample units measured in multiple years, and this might utilize model-based updating techniques.

Current Statistical Methods for Annual FIA Inventories

The annual FIA design is organized around a system of 5 "panels" (*i.e.*, independent sub-samples) in the eastern USA and 10 panels in the western USA. A panel is a systematic sub-sample of all permanent FIA primary sampling units (Phase-2, or "P2", field plots) for which field measurements are conducted on 2 or more occasions. Each FIA panel is composed of a spatially balanced, systematic, interpenetrating sub-sample of all FIA field plots (Reams and others, 2005). In simple terms, FIA treats each panel of field plots as an independent, equal-probability sample of the entire population. All FIA field plots in the first panel are measured during the course of 1 or more years[3]. After essentially all plots in the first panel are measured, field measurements of the second panel commence. Afterwards, the 3rd panel is measured, and so forth for the remaining panels. This sequence of field plot measurements is repeated over time until all FIA panels are measured. This typically takes 5 to 10 years, depending on the region of the country and available funding. After the initial 5 to 10 years, this same sequence

[3] The annual FIA design originally envisioned measurement of a single panel within a single calendar year. However, within the limits of available funds, it often requires more than 12 months to measure a single panel. This is termed "panel creep."

of annual panel measurements is repeated in subsequent time periods. The result is a cyclic time-series of cross-sectional and longitudinal sample survey observations of the population from independent panels of FIA field plots. FIA does not use split or overlapping panels (Kish 1987).

FIA does not currently have an officially endorsed estimator that combines multiple panel data to improve statistical precision, and it has not yet been determined if any single estimator will be fully satisfactory for all regions and forest conditions (Patterson and Reams 2005). FIA is currently investigating the Moving Average, the Temporally Indifferent Method and model-based estimators The latter includes mixed estimators (*e.g.*, Van Deusen 2002), Kalman filters (*e.g.*, Brockwell and Davis 1996), and various time series models (*e.g.*, Johnson and others 2003). The Moving Average and the Temporally Indifferent methods are relatively straightforward, and they closely resemble the estimators used by FIA during the past half-century for periodic inventories (Scott and others 2005, Patterson and Reams 2005).

Patterson and Reams (2005) discuss a simple approach to monitoring change. The net difference between 2 sequential, but different, panels is one simple estimate of change. Since each sequential panel is an independent sample by design, the variance of the difference is the sum of the variances from each of the 2 panels. Over time, annual estimates of the net differences produce a series of annual estimates for change. However, estimates for the components of net change require re-measurement of FIA plots, which occurs after all annual panels are measured for the first time (i.e., after 5 to 10 years). Also, variance of the net difference can be large at the scale of a state or smaller sub-populations, resulting in considerable uncertainty.

The remainder of this section provides more detail on the Moving Average and Temporally Indifferent methods[4]. Later sections look at the Kalman filter as an example of a model-based time-series estimator.

Moving Average Method: Patterson and Reams (2005) describe the moving average method as follows. *"Let P denote the number of panels to be combined for analysis. Let Y_p denote the true quantity for panel P, where p=1,…,P; and let $\hat{Y}_p$ denote the estimate of Y_p obtained using the appropriate technique from Scott and others (2005). Note that each panel is treated as an independent estimate, which permits (1) the weighting of individual panels; and (2) Phase 1 stratification instruments to differ among panels (i.e., different maps may be used to stratify different panels)."* The Moving Average estimator is given by Patterson and Reams (2005) and Roesch and Reams (1999) as:

[4] The Moving Average and Temporally Indifferent methods are implicitly "model-based" if the assumption is that they are estimators of the current conditions at time t=1 in equation 1.

$$\hat{Y}_{MA,P} = \sum_{p=1}^{P} w_p \hat{Y}_p \quad \text{where} \sum_{p=1}^{P} w_p = 1 \qquad [1]$$

The panel measured most recently is denoted p=1, and panels measured at previous P time periods have values p=2,…,P. Patterson and Reams recommend equal weighting of panels, *i.e.*, $w_p=1/P$ for all p. They give the variance estimator for the Moving Average as the corresponding weighted sum of the variances for each panel estimate p:

$$V\left[\hat{Y}_{MA,P}\right] = \sum_{p=1}^{P} w_p^2 \, V\left[\hat{Y}_p\right] \qquad [2]$$

Patterson and Reams remark that the Moving Average dampens annual fluctuations in the estimates, and estimated changes in the population tend to appear smaller than their true values. The Moving Average can cause a "lag bias" when the population is not at a static steady state, and this can obscure trends over time (Roesch and Reams 1999). However, lag bias can be inconsequential unless there is a rapid, widespread catastrophic event (Johnson and others 2003).

Moving Average Residuals: The residual difference r_{MA} between the estimator for the current panel and the moving average for the last P panels might be used to test the hypothesis that the population is at relative steady state (*i.e.*, $Y_1 = Y_{MA,P}$) If this hypothesis is rejected, then there is empirical evidence from the FIA sample that the population measured with panel p=1 does not equal the population moving average over the most recent P panels, *i.e.*, the population has changed somehow during the last P panel measurements. The variance estimator for the residual difference equals:

$$\begin{aligned}
\mathrm{Var}\left(\hat{Y}_1 - \hat{Y}_{MA,P}\right) &= \mathrm{Var}\left(\hat{Y}_1\right) + \mathrm{Var}\left(\hat{Y}_{MA,P}\right) + 2\sum_{p=1}^{P} \mathrm{Cov}\left(\hat{Y}_1, \frac{-1}{P}\hat{Y}_p\right) \\
&= \mathrm{Var}\left(\hat{Y}_1\right) + \mathrm{Var}\left(\hat{Y}_{MA,P}\right) + \frac{-2}{P}\mathrm{Var}\left(\hat{Y}_1\right) \quad \begin{cases} \mathrm{Cov}\left(\hat{Y}_1, \hat{Y}_{p|p\neq 1}\right) = 0 \\ \mathrm{Cov}\left(\hat{Y}_1, \hat{Y}_1\right) = \mathrm{Var}\left(\hat{Y}_1\right) \end{cases} \\
&= \left(1 - \frac{2}{P}\right)\mathrm{Var}\left(\hat{Y}_1\right) + \mathrm{Var}\left(\hat{Y}_{MA,P}\right)
\end{aligned} \qquad [3]$$

The difference between the design-based estimator $\hat{Y}_1$ for the single panel at time t=1 and the Moving Average $\hat{Y}_{MA,P}$ over panels p=1,…,P may be standardized relative to the estimated standard deviation of the difference from equation 3:

$$r_{MA} = \frac{\hat{Y}_1 - \hat{Y}_{MA,P}}{\sqrt{\mathrm{Var}\left(\hat{Y}_1 - \hat{Y}_{MA,P}\right)}} \qquad [4]$$

Given the hypothesis Y_1=$Y_{MA,P}$ in equation 4, r_{MA} has an expected value of 0 with an expected standard deviation of 1 (i.e., unit variance). Assuming the residuals have a normal distribution, there is a 32 percent probability that a standardized residual be less than -1 or greater than +1, and a probability of merely 5 percent that it will be less than -1.96 or greater than +1.96.

A simple metric for the relative efficiency of the Moving Average is its variance relative to the variance for the most current panel (p=1):

$$\beta = \frac{\mathrm{Var}\left(\hat{Y}_{MA,P}\right)}{\mathrm{Var}\left(\hat{Y}_1\right)} \qquad [5]$$

β will generally range between 0 and 1 because the estimated variance of the Moving Average is usually, but not necessarily, less than the estimated variance for any one panel being averaged. The standardized residual r_{MA} in equation 4, and the gain in statistical efficiency β in equation 5, subsequently will be used to directly compare the Moving Average with the Kalman filter.

Temporally Indifferent Method: Patterson and Reams (2005) describe the Temporally Indifferent Method, which is very similar to the Moving Average. Sampling units in all *panels* (p=1,…,P) are pooled as though they were all part of a single large periodic inventory. As with previous FIA periodic inventories, Phase 1 post-stratification is applied across sampling units from all P panels. If the number of sampling units is virtually the same in each panel, and a single source of remotely sensed data are used for post-stratification within each panel, then the Temporally Indifferent Method is algebraically equivalent to the (Moving Average).

Summary: The Moving Average and Temporally Indifferent estimators are simple, and simplicity can be good. The Temporally Indifferent estimator can be applied with the same familiar approach previously used for decades with periodic FIA surveys, and familiarity can be good. The Moving Average and Temporally Indifferent estimators produce useful inventory estimates for the current state of the nation's forests, which are updated annually as new panel data are acquired. However, these simple and familiar methods have inherent limitations in the context of estimation and interpretation of changes over time, which is necessary to address the substantive monitoring questions identified in the FIA strategic plan (U.S. Forest Service 2007a).

An Alternative Estimator for Monitoring

In addition to the Moving Average and Temporally Indifferent methods, Patterson and Reams (2005) list model-based time-series methods as alternative estimation methods that can combine FIA panel estimates over time. Van Deusen (1999) reviews sampling with partial replacement methods, although those have concentrated on periodic surveys. One promising approach for panel data is the mixed estimator (Theil 1971), which has been studied by Van Deusen (1999, 2002, 2008) and Roesch (1999, 2007, 2008) for applications to annual forest inventory and monitoring. In addition, Patterson and Reams (2005) cite Czaplewski (1995) and Brockwell and Davis (1996), who discuss the Kalman filter (see Maybeck 1979) as another alternative. As discussed below, the Kalman filter combines the advantages of model-based and design-based estimators to mitigate risk while reliably improving statistical efficiency.

The remainder of this paper concentrates on the Kalman filter, which has been widely used in engineering applications for 50 years to estimate the states of a system over time. However, the Kalman filter is not well-known in forest inventory and monitoring applications[5]. The Kalman filter is conceptually intuitive, which, hopefully, will soon become apparent. With this goal in mind, the following exposition begins with the univariate Kalman filter, which uses as its basic building block a well known and simple statistical method, namely, the composite estimator.

Composite Estimator

The Kalman filter may be viewed as the sequential application of the composite estimator (Gregoire and Walters 1988). Maybeck (1979) is an often cited and well written source on the Kalman filter. He begins his 3-volume seminal treatise on the Kalman filter with a simple example of the composite estimator, which may also be considered an example of the static Kalman filter. The following is a slightly modified reproduction of Maybeck's introduction from his section 1.5 in Volume 1:

"Suppose that you are lost at sea during the night and have no idea at all of your location. So you take a star sighting to establish your position (for the sake of simplicity, consider a 1-dimensional location). At some time t_1 you determine your location to be z_1. However, because of inherent measuring device inaccuracies, human error, and the like, the result of your measurement is somewhat uncertain. Say you decide that the precision is such that the standard deviation (1-sigma value) involved is σ_{z_1} (or equivalently, the variance or second

[5] For exceptions, see Dixon and Howitt 1979; Gregoire and Walters 1988; Walters and others 1991; Visser and Molenaar 1992; Czaplewski 1995; Van Deusen 1987, 1989; Devall and others 1991; Brakel and Visser 1996; Gove and Houston 1996; Williams and others 2005; Hurteau and others 2007; Gao and others 2008.

order statistic, is $\sigma^2_{z_1}$ *). Thus, you can establish the conditional probability of* $x(t_1)$*, your position at time* t_1 *conditioned on the observed value of the measurement being* z_1*, as depicted in* (figure 1). *This is a plot of* $f_{x(t_1)|z(t_1)}(x|z_1)$ *as a function of the location x: it tells you the probability of being in any 1 location, based upon the measurement you took. Note that* σ_{z_1} *is a direct measure of the uncertainty: the larger* σ_{z_1} *is, the broader the probability peak is, spreading the probability "weight" over a larger range of x values. For a Gaussian density, 68.3% of the probability "weight" is contained within the band σ units to each side of the mean, the shaded portion in* (figure 1).

"Based on this conditional probability density, the best estimate of your position is

$$\hat{x}(t_1) = z_1 \tag{6}$$

and the variance of the error in the estimate is

$$\sigma_x^2(t_1) = \sigma_{z_1}^2 \tag{7}$$

"Note that $\hat{x}$ *is both the mode (peak) and the median (value with 1/2 of the probability weight to each side), as well as the mean (center of mass).*

"Now say a trained navigator friend takes an independent fix, right after you do, at time $t_2 \sim t_1$ *(so that the true position has not changed at all, and obtains a measurement* z_2 *with a variance* $\sigma_{z_2}^2$*. Because he has a higher skill, assume the variance in his measurement to be somewhat smaller than yours.* Figure 2 *presents the conditional density of your position at time* t_2*, based only on the measured value* z_2*. Note the narrower peak due to smaller variance, indicating that you are rather more certain of your position based on his measurement.*

"At this point, you have 2 measurements available for estimating your position. The question is, how do you combine these data? It will be shown subsequently that, based on the assumptions made, the conditional density of your position at time $t_2 \sim t_1$*,* $x(t_2)$*, given* both z_1 and z_2*, is a Gaussian density with mean* μ *and variance* σ^2 *as indicated in* figure 3*, with*

$$\mu = \left(\frac{\sigma_{z_2}^2}{\sigma_{z_1}^2 + \sigma_{z_2}^2} \right) z_1 + \left(\frac{\sigma_{z_1}^2}{\sigma_{z_1}^2 + \sigma_{z_2}^2} \right) z_2 \tag{8}$$

$$\frac{1}{\sigma_\mu^2} = \frac{1}{\sigma_{z_1}^2} + \frac{1}{\sigma_{z_2}^2} \tag{9}$$

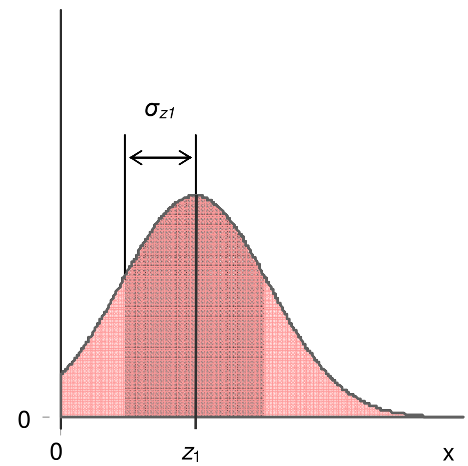

Figure 1: Conditional density of position based on measured value z_1 (facsimile of figure 1.4 in Maybeck 1979). The distribution extends to both ±∞, but it is truncated in this illustration.

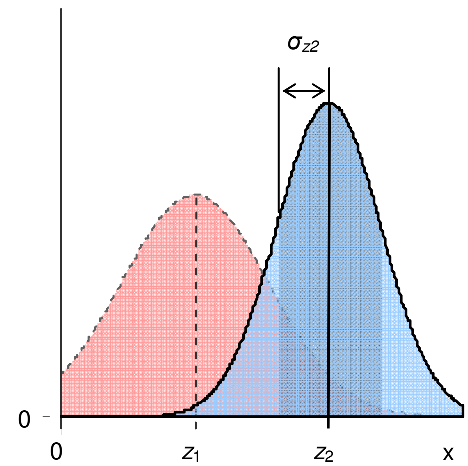

Figure 2: Conditional density of position based on measurement z_2 alone (facsimile of figure 1.5 in Maybeck 1979).

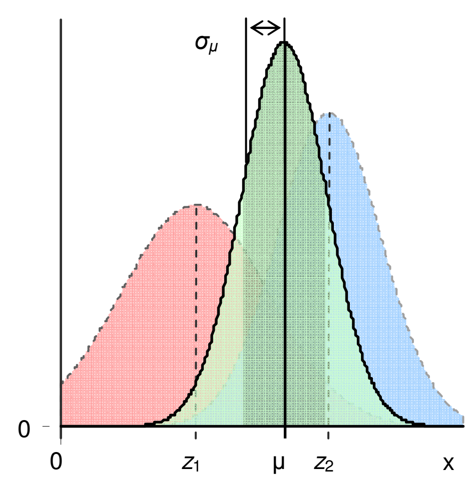

Figure 3: Conditional density of position based on data z_1 and z_2 (facsimile of figure 1.6 in Maybeck 1979).

*"Note that, from (*equation 9), *σ_μ is less than either σ_{z1} or σ_{z2}, which is to say that the uncertainty in your estimate of position has been decreased by combining the 2 pieces of information.*

"Given this density, the best estimate is

$$\hat{x}(t_2) = \mu \qquad [10]$$

with an associated error variance σ^2. It is the mode and the mean (or, since it is the mean of a conditional density, it is also termed the conditional mean). Furthermore, it is also the maximum likelihood estimate, the weighted least squares estimate, and the linear estimate whose variance is less than that of any other linear unbiased estimate.[6] *In other words, it is the "best" you can do according to just about any reasonable criterion.*

"After some study, the form of μ given in (equation 8) *makes good sense. If σ_{z1} were equal to σ_{z2}, which is to say you think the measurements are of equal precision, the equation says the optimal estimate of position is simply the average of the 2 measurements, as would be expected*[7]. *On the other hand, if σ_{z1} were larger than σ_{z2}, which is to say that the uncertainty involved in the measurement z_1 is greater than that of z_2, then the equation dictates "weighting" z_2 more heavily than z_1. Finally, the variance of the estimate is less than σ_{z1} even if σ_{z2} is very large: even poor quality data provide some information, and should thus increase the precision of the filter output.*

"The equation for $\hat{x}(t_2)$ can be rewritten as

$$\begin{aligned} \hat{x}(t_2) &= \left(\frac{\sigma_{z_2}^2}{\sigma_{z_1}^2+\sigma_{z_2}^2}\right) z_1 + \left(\frac{\sigma_{z_1}^2}{\sigma_{z_1}^2+\sigma_{z_2}^2}\right) z_2 \\ &= z_1 + [z_2 - z_1]\left(\frac{\sigma_{z_1}^2}{\sigma_{z_1}^2+\sigma_{z_2}^2}\right) \end{aligned} \qquad [11]$$

or, in final form that is actually used in Kalman filter implementations [noting that $\hat{x}(t_1) = z_1$]

$$\begin{aligned} \hat{x}(t_2) &= \hat{x}(t_1)(1-\beta) + z_2\beta \\ &= \hat{x}(t_1) + [z_2 - \hat{x}(t_1)]\beta \end{aligned} \qquad [12]$$

---

[6] The Kalman filter may also be derived as an Empirical Bayes estimator (Jazwinski 1970, Meinhold and Singpurwalla 1983, Cressie and Wikle 2002).

[7] This is the same assumption made in the FIA Moving Average (Patterson and Reams 2005), namely, each estimate from the last *P* panels is equally accurate in estimating the current condition of the population (or the condition at the time panel *p*=*P*/2 was sampled).

where[8]

$$\beta = \frac{\sigma_{z_1}^2}{\sigma_{z_1}^2 + \sigma_{z_2}^2}$$

$$= \frac{\sigma_x^2(t_1)}{\sigma_x^2(t_1) + \sigma_{z_2}^2} \qquad [13]$$

"These equations say that the optimal estimate at time t_2, $\hat{x}(t_2)$, *is equal to the best prediction of its value before* z_2 *is taken,* $\hat{x}(t_1)$, *plus a correction term of an optimal weighting value times the difference between* z_2 *and the best prediction of its value before it is actually taken,* $\hat{x}(t_1)$. *It is worthwhile to understand this "predictor-corrector" structure of the filter. Based on all previous information, a prediction of the value that the desired variables and measurement will have at the next measurement time is made. Then, when the next measurement is taken, the difference between it and its predicted value is used to `correct' the prediction of the desired variables.*

"Using the β … *in* (equation 13)*, the variance equation given by* (equation 9) *can be rewritten as*

$$\sigma_x^2(t_2) = \sigma_x^2(t_1) - \sigma_x^2(t_1)\beta \qquad [14]$$

"Note that the values of $\hat{x}(t_2)$ *and* $\sigma_x^2(t_2)$ *embody all of the information in* $f_{x(t_2)|z(t_1),z(t_2)}(x|z_1, z_2)$. *Stated differently, by propagating these 2 variables, the conditional density of your position at time* t_2, *given* z_1 *and* z_2, *is completely specified.*

"Thus we have solved the static estimation problem."

Hopefully, Maybeck's example provides intuitive insight into the simplicity, efficiency, and flexibility of the composite estimator, which is a special case of the Kalman filter.

[8] The symbol "*β*" is used in place of Maybeck's "*K*" to draw the analogy to regression estimators in sample surveys (e.g., Sarndäl and others 1992).

Model-Based Bias with the Composite Estimator

If estimators z_1 and z_2 for population parameter z are both unbiased by design, then the composite estimator, which is a weighted sum of z_1 and z_2, will be design-unbiased. However, the Kalman filter generally assumes that z_1 is based on an estimate from the previous time period, which is "updated" with a prediction model into an estimate for the state of the population at the current time period, namely $z_1=x(t_1)$. This model-based component has the potential to substantially improve precision of the composite estimator, but accuracy can be poor if the model produces biased predictions. In most applications, the model requires assumptions that are difficult to test. Therefore, special attention is required to detect and correct failures in model assumptions, which is the topic of this section. Otherwise, the composite estimator can produce estimates that are apparently very precise, but are, in fact, very inaccurate (*i.e.,* biased).

Successful applications of the Kalman filter require close monitoring of the residual difference between $x(t_1)$ and z_2 to detect likely bias in model predictions (Maybeck 1979). Denote this residual as

$$r(t_2) = \hat{z}_2 - \hat{x}(t_1) \tag{15}$$

Assuming independence, the expected variance of this residual is:

$$\sigma_r^2(t_2) = \sigma_{z_2}^2 + \sigma_x^2(t_1) \tag{16}$$

A useful monitoring technique requires standardization of this residual based on its expected variance. If the model is an unbiased estimator, then the standardized residual in equation 17 is expected to have a distribution with mean zero and unit variance:

$$\frac{r(t_2)}{\sqrt{\sigma_r^2(t_2)}} \sim (0,1) \quad \left| \begin{array}{l} \text{given unbiased} \\ \text{model-based estimator} \\ x(t_1) \text{ and } \sigma_x(t_1) \end{array} \right. \tag{17}$$

At each time step, assume there is a known model-based prediction of $x(t_1)$ with a known model-based estimate of its variance. Further assume there is a known design-based panel estimate z_2 with a known design-based estimate of its variance. Under these assumptions, the residual may be computed with equation 15, the predicted variance of this residual may be computed with equation 16, and the resulting residual may be standardized as in equation 17.

One process to monitor the reliability of the model-based estimator is with the "size" of this standardized residual. Assuming the standardized residual is normally (Gaussian) distributed, with mean zero and unit variance (*i.e.*, variance equal to 1 in equation 17), then there is a 68.3 percent probability that the standardized residual will be between -1 and +1, and a 95.4 percent probability that it will be between −2 and +2.

Figure 4A provides an example, in which the standardized residual equals 1, and the standardized residual is assumed normally distributed with mean zero and unit variance. When monitoring residuals under these assumptions, a standardized residual as large as 1 is not too surprising because 31.7 percent (*i.e.*, 1.000-0.683= 0.317) of all residuals are expected to be less than −1 or greater than +1.

As an aside, this example also illustrates that the distribution of random errors in the design- and model-based estimators need not be assumed to be Gaussian normal. Figure 4 assumes a lognormal distribution, in which feasible variables may not have negative values. However, the residual difference between 2 estimates may have a negative value if the model-based estimate exceeds the design-based panel estimate. Therefore, the distribution of standardized residuals may be assumed Gaussian normal, although that is nothing more than another untested assumption.

Figure 4B is another example, in which the model-based estimate is greater than that in figure 4A, but it otherwise shares the same parameter values as those in figure 4A. In this example, the standardized residual equals 2. Under the assumptions in this example, the probability of a standardized residual less than −2 or greater than +2 is only 4.6 percent. This is a relatively low probability, but observation of a residual of this magnitude remains plausible under the assumptions of the residual analysis.

Figures 4C and 4D are more extreme examples. Again, under the assumptions in this analysis of residuals, the probability of the absolute value of the standardized residual exceeding the value of 3 is 0.3 percent in figure 4C, and of exceeding the value 4 in figure 4D is 0.006 percent. Both are evidence that 1 or more assumptions in the residual analysis are suspect. Since the panel estimate z_2 is design-unbiased, the assumptions related to this estimator remain credible, at least in the absence of substantial non-sampling errors. It is more plausible that 1 or more assumptions related to the model-based estimator $x(t_1)$ are incorrect.

The model-based estimate might be biased. However, if the magnitude of the bias is quantitatively predictable, then the model should include a correction term that corrects for the bias. In other words, a model with a bias that could be estimated should not be knowingly used in the Kalman filter. Rather, the bias correction should be incorporated into the base model.

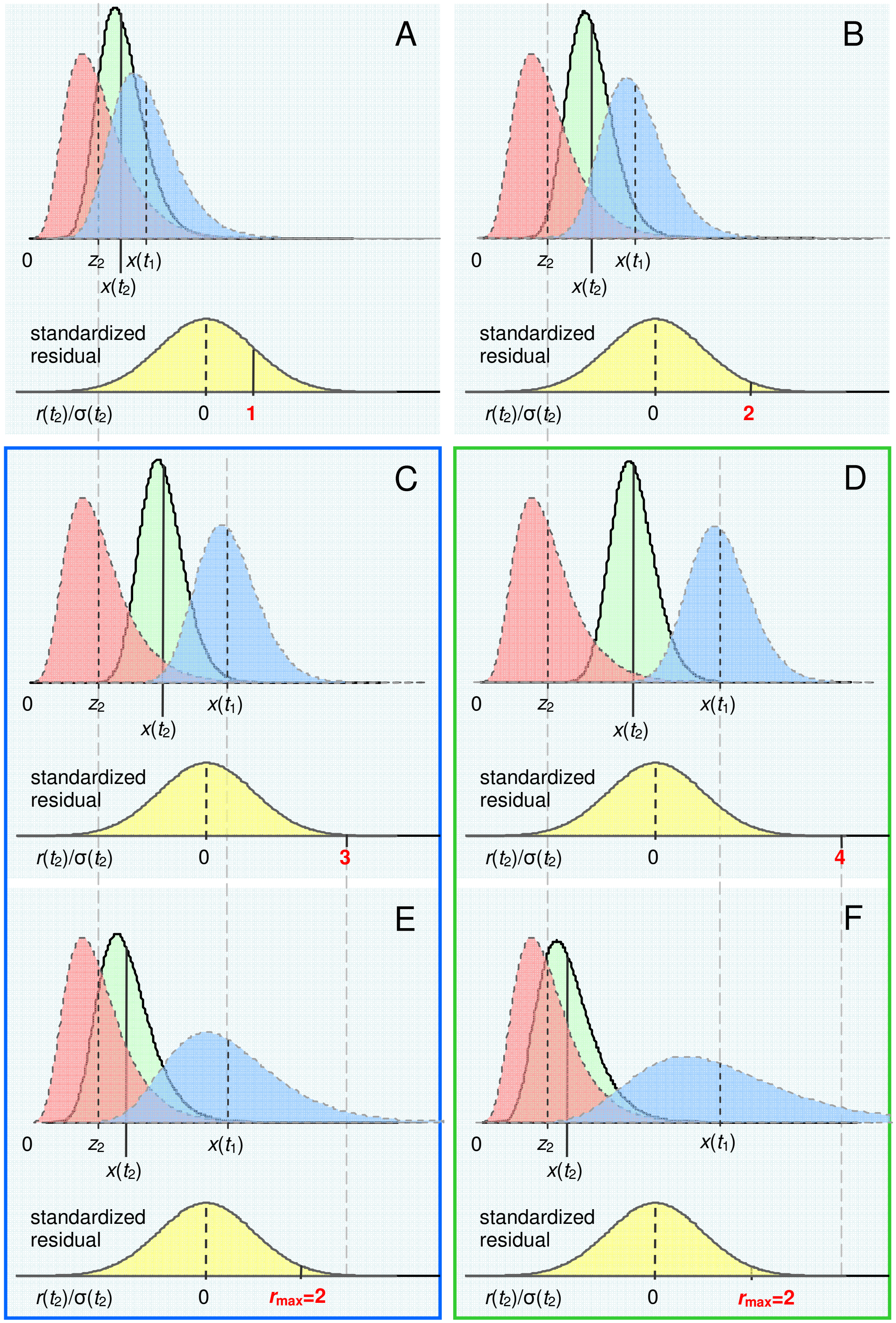

Figure 4: Reliable applications of the composite estimator with a model-based component, which is a special case of the static Kalman filter, requires monitoring residuals and adapting to evidence that the model assumptions are significantly flawed.

The other suspect is the estimated variance of random prediction errors with the model, namely $\sigma_x^2(t_1)$. This variance can be difficult to accurately estimate from *a priori* empirical data when the number of residuals is small or the variance is heteroscedastic over time. One solution would be to assume the model-based variance estimator is biased, and re-estimate its variance so that the realized magnitude of the standardized residual is more plausible given the design-based estimate from the most current FIA panel.

One *ad hoc* adjustment rule could be to increase the estimated variance of the model-based estimator by a scalar factor of *c* so that the absolute value of its standardized residual becomes a more plausible value, say $r_{\max}$. This assures that the standardized residuals never exceed $\pm r_{\max}$ standard deviation units. For example, if $r_{\max}=2$, then the residual difference between the model-based and design-based estimates would be forced to remain within 2 standard deviation units of 0.

From equations 16 and 17 and this rule, it will be assumed that a less biased estimator for the variance of model prediction errors is $c\sigma_x^2(t_1)$, which is computed as:

$$\frac{|r(t_2)|}{\sqrt{\sigma_{z_2}^2 + c\sigma_x^2(t_1)}} \le |r_{\max}|$$

$$c\sigma_x^2(t_1) = \left(\frac{r(t_2)}{r_{\max}}\right)^2 - \sigma_{z_2}^2 \qquad [18]$$

Figure 4F is an example in which this *ad hoc* solution is applied to the statistics from figure 4D. In figure 4D, the standardized residual has the value of 4 standard deviation units. The variance of the estimator for $x(t_1)$ is re-estimated with equation 18, where the maximum plausible value of the standardized residual is chosen to be $r_{\max}=2$, namely, 2 standard deviation units. This increases the estimated variance of the model prediction error, resulting in a new standardized residual exactly equal to $r_{\max}=2$, which, in turn, increases the value of β in equation 13, which decreases the relative “weight” placed on the model prediction in equation 12. The outcome is a composite estimate that more closely agrees with the design-based estimator of z_2. The new composite estimate in figure 4F has a larger variance estimate than the composite estimate in figure 4D, but the estimate in figure 4F will be closer to the true value if the new assumptions in the model become more accurate. Figure 4E, which has a standardized residual equal to 3 standard deviation units, is a less extreme example relative to figure 4F.

In summary, the model-based composite estimator can be very efficient, but it can also be dangerously biased if the model is inaccurate. Since model parameters are typically fit with historical data, substantial deviations of a population from its historical conditions will likely cause biased model predictions. Statistical efficiency has an associated risk. There is nothing inherent within the composite estimator, and therefore, within the Kalman filter, that protects against model-based bias[9]. Monitoring residuals and adapting to anomalous outcomes can mitigate the risk of serious bias without foregoing the opportunities for increased efficiencies. Kott (2005) advocates a similar view in his paper on randomization-assisted model-based survey sampling

Kalman Filter Estimator

The Kalman filter can be viewed as the sequential application of the composite estimator for each encounter of new information. In monitoring changes and trends over time with sub-sampled FIA panel data, the first component $z(t)$ is the design-based estimator for the most current FIA panel (Scott and others 2005). The second component $x(t|t-1)$ is a model-based estimator that uses the best FIA estimate from the previous year ($t-1$), which is updated to year t with a model for predicted change between years t and $t-1$. The Kalman filter is simply the sequential application, 1 year at a time (t=1,2,…), of this composite estimator and its underlying model.

Recall from Maybeck's introduction (page 6) that the composite estimator is the simple weighted sum of $x(t|t-1)$ and $z(t)$ (see also Sarndäl and others 1992, section 9.9.1). Using primarily Maybeck's notation in the context of the univariate time-series (equation 12), the composite estimator $x(t|t)$ at time t is the weighted sum of the FIA panel estimator $z(t)$ at time t and the model-based predictor $x(t|t-1)$ of the same population parameter at time t given the composite estimator at time $t-1$:

$$\left.\begin{aligned}\hat{x}(t|t) &= (1-\beta_t)\hat{x}(t|t-1) + \beta_t \hat{z}(t) \\ &= \hat{x}(t|t-1) + \left[\hat{z}(t) - \hat{x}(t|t-1)\right]\beta_t\end{aligned}\right\} \quad \text{where } 0 \le \beta_t \le 1 \qquad [19]$$

The "optimal" weight ($1-\beta_t$) placed on the model estimate (equations 12 and 13) at time t is:

$$\begin{aligned}(1-\beta_t) &= \frac{\sigma_z^2(t)}{\sigma_x^2(t|t-1)+\sigma_z^2(t)} \\ \beta_t &= \frac{\sigma_x^2(t|t-1)}{\sigma_x^2(t|t-1)+\sigma_z^2(t)}\end{aligned} \qquad [20]$$

The variance estimator for equation 19, which is the time-series version of equations 9 and 13, is algebraically equivalent to the following expressions:

---

9 There is nothing to protect against similar bias with the Moving Average or Temporally Indifferent methods (Roesch, personal communication).

$$
\begin{aligned}
\sigma_x^2(t|t) &= (1-\beta_t)^2\sigma_x^2(t|t-1) \;+\; \beta_t^2\sigma_z^2(t) \\
&= \frac{\sigma_z^2(t)\sigma_x^2(t|t-1)}{\sigma_x^2(t|t-1)+\sigma_z^2(t)} \\
&= \sigma_x^2(t|t-1)-\beta_t\sigma_x^2(t|t-1) \\
&= \beta_t\sigma_z^2(t)
\end{aligned}
\qquad [21]
$$

The weight β_t in equation 21 is algebraically equivalent to the scalar reduction in the variance of the design-based panel estimator at time *t* given the model-based estimate at time *t*. This is analogous to the "design effect" used to evaluate efficiency of different sampling designs (Maybeck 1979).

The time-series model in the Kalman filter assumes the population total $x(t)$ at time *t* equals the total $x(t-1)$ at $t-1$, which is multiplied by the scalar rate of change (φ_t) between *t* and $t-1$. This is the difference equation:

$$x(t) = \varphi_t \; x(t-1) + \varepsilon_w(t) \qquad [22]$$

where $\varepsilon_w(t)$ in equation 22 represents the unknown random prediction error from time $t-1$ to *t*. The model assumes $\varepsilon_w(t)$ is distributed with mean zero and variance $\sigma_w(t)$. The corresponding model-based predictor for use in the Kalman filter is:

$$\hat{x}(t|t-1) = \varphi_t \; \hat{x}(t-1|t-1) \qquad [23]$$

$$\sigma_x^2(t|t-1) = \varphi_t^2 \; \sigma_x^2(t-1|t-1) \;+\; \sigma_w^2(t) \qquad [24]$$

In successful applications of the Kalman filter, estimates for the standard deviation of model-based predictions $\sigma_w(t)$ are carefully monitored through the realized residuals and adapted if necessary (see above).

Sequential Recursive Time-Series Estimation with the Kalman Filter

The following example is intended to explain in a more intuitive fashion an application of the Kalman filter for FIA monitoring. Assume a temporal model predicts the population parameter *x* is exponentially increasing over the time period being analyzed. More specifically, assume, φ_t = 1.5 in equations 23 and 24. Assume the random prediction error over a single year (equation 22) has a heteroscedastic standard deviation equal to 0.25 times the population parameter *x* at time *t*. In prose, the model assumes that the population parameter increases 50 percent each year relative to its value at the previous year, and the random prediction error of this model has a standard deviation of ±25 percent at time t relative to its condition at $t-1$ for all t. With these specific assumptions, the model-based estimator at time t is specified from equations 23 and 24 as:

$$\hat{x}(t|t-1) = \left(\frac{3}{2}\right) \times \hat{x}(t-1|t-1) \tag{25}$$

$$\sigma_x^2(t|t-1) = \left[\left(\frac{3}{2}\right)^2 \times \sigma_x^2(t-1|t-1)\right] + \left[\left(\frac{1}{4}\right) \times x(t-1|t-1)\right]^2 \tag{26}$$

Assume an FIA panel (*i.e.*, sub-sample) is measured at time t=1. The design-based estimate of $x(1|1)$ is produced with standard FIA methods as given by Scott and others (2005). Given this model, figure 5 illustrates how these initial conditions are predicted to change over time in the absence of any further FIA data at times t=2,…,6. The model in equation 25 forecasts that the population parameter will increase exponentially, and the model in equation 26 predicts the uncertainty of this forecast increases nonlinearly over time. The random error distributions are assumed to the skewed lognormal, similar to figure 4, in which negative values are infeasible. Since the Kalman filter is a minimum variance estimator, it does not necessarily depend on the assumption of Gaussian normal or symmetric error distributions.

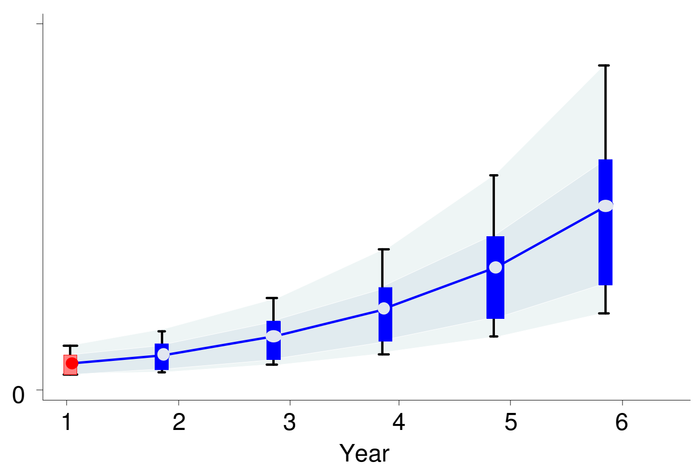

Figure 5: Predictions of the population parameter and the associated uncertainty (standard deviation) from the model in equations 25 and 26 in the absence of new FIA panel estimates at times t=2,…,6.. The initial condition at time t=1, which is portrayed by the red box plot, is the standard FIA design-based estimate from a single panel (Scott and others 2005). The subsequent model-based estimates are illustrated by the blue box plots. The model assumes the random sampling and prediction errors have a lognormal distribution to assure that negative values are infeasible.. The range of the boxes is the 25th and 75th percentiles, and the range of the "whiskers" is the 10th and 90th percentiles.

This model is the component of the Kalman filter that links the time series of observations over time. Using the simple composite estimator, the Kalman filter combines the observation at time *t* with the model prediction at time *t* to produce a more accurate estimate at time *t*.

The Kalman filter produces a composite estimate at a single time *t* based on any direct observations of the population at time *t* (e.g., a design-based estimate from a single FIA panel) plus the independent model forecast of the same population parameter at time *t* (e.g., equations 25 and 26, figure 5). This forecast uses the best estimate of the population parameter at time $t-1$ as initial conditions. The resulting composite estimate embodies the information available in all observations and model predictions up to and including time *t*. The next operation in the Kalman filter sequence uses this best estimate at time *t* to forecast the state of the population at the subsequent time step $t+1$, and the composite estimator combines this forecast with any new independent observations at time $t+1$ into a more accurate estimate at time $t+1$. And so forth. Figure 6 provides an example.

The red box plots represent the 10^{th}, 25^{th}, 50^{th}, 75^{th} and 90^{th} percentiles of the assumed lognormal distribution of sampling errors in the estimate of the population attribute. This means that 10 percent of the assumed distribution exceeds the upper whisker on the box plot, and another 10 percent is less than the lower whisker. Thus, there is only about 80 percent of the distribution covered by the range of each box plot.

Simulated Examples of Monitoring Trends over Time

This section provides a variety of examples that compare Kalman filter and Moving Average estimates. The "true" population value at each time *t* is known exactly because they were used to generate the simulated estimates from each panel[10].

The following examples provide a range of departures of the "real world" from the assumed model in the Kalman filter, which reveals examples of the consequences of those departures on the reliability of annual estimates. However, these examples are merely specific realizations. They do not provide valid generalizations about bias or efficiency of the estimators. Such generalizations require deriving their expected values over all possible samples, or at least a very large number of potential samples.

10 While the true values in these hypothetical populations may be known during these simulations, the true values are not known in FIA sampling and estimation of forest populations.

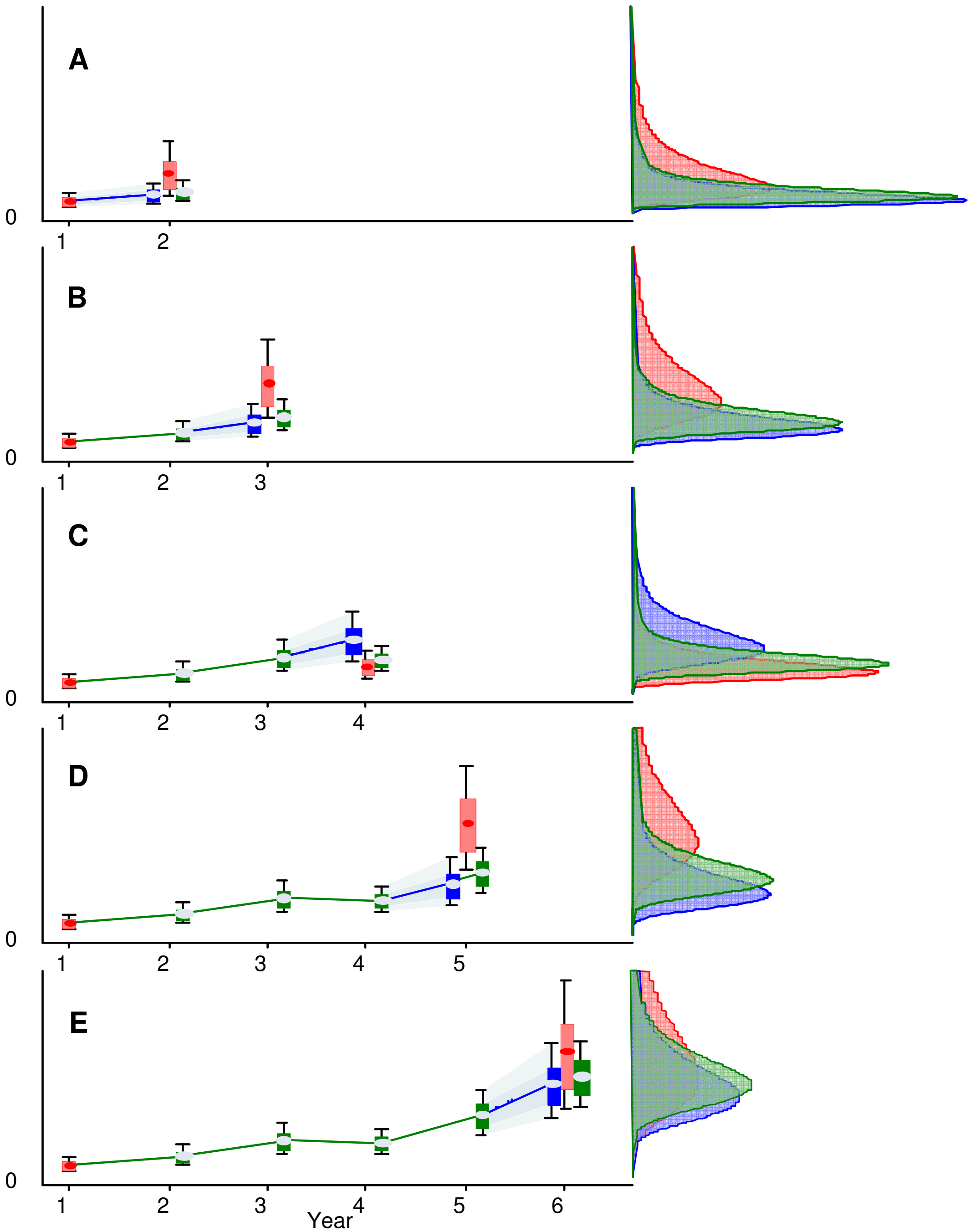

Figure 6: An example of the sequential recursive nature of the Kalman filter. Start with figure 6A. The design-based panel estimate at time *t*=2 is denoted with the red box plot. The model-based estimate (denoted with the blue box plot) is an independent forecast for time *t*=2 based on the best estimate at time *t*=1 (see equations 25 and 26, figure 5). The Kalman filter is the composite estimate (denoted with the green box plot) of these design- and model-based estimates. Figure 6B illustrates the next sequential step at time *t*=3, which uses the same process in the Kalman filter as that at time *t*=2. The design-based estimate at time *t*=1 is no longer needed at time *t*=3 because its contribution to the *t*=3 estimate is completely captured in the Kalman filter estimate at time *t*=2. Figures 6C, 6D and 6E illustrate subsequent steps in this sequential process. Conditional lognormal error distributions on the right-hand side supplement the box plots use the same color convention as in figure 5, where each box plot portrays the 10th, 25th, 50th, 75th, and 90th percentiles of the modeled distributions.

For sake of simplicity and generality, the model chosen for this section makes few prior assumptions about the simulated dynamics of the populations. Assume a temporal model in the Kalman filter that predicts that the population parameter x is at a constant (static) steady-state over time, i.e., $\varphi_t = 1$ in equations 23 and 24. Assume the random prediction error over a single year (equation 22) has a relatively small but heteroscedastic standard deviation equal to 0.05 times the population parameter x at time t. In prose, the model assumes that the population is nearly at a constant steady-state that has minor random variations each year around a long-term constant value. The model for the standard deviation of this natural random variation is ±5 percent at time t relative to its condition at t−1 for all t. Under these assumptions, the model-based estimator at time t, which is a specific case of the general models in equations 23 and 24, is defined as:

$$\hat{x}(t|t-1) = \hat{x}(t-1|t-1) \tag{27}$$

$$\sigma_x^2(t|t-1) = \sigma_x^2(t-1|t-1) + \left[0.05 \times x(t-1|t-1)\right]^2 \tag{28}$$

This particular model in the Kalman filter (equations 27 and 28) approximately matches the model implied by the Moving Average, namely, estimates with the Moving Average are reliable for the current year if there is negligible change in the population over the time period being averaged.

The first example employs a simulated population that is at a true steady-state, in which there is no change over time. A single realization of a simulated sample from this population is given in figure 7A, in which the design-based sampling errors (red box plots) have a coefficient of variation of 15 percent. Figure 7B illustrates a second independent realization, in which the design-based sampling errors have a coefficient of variation of 30 percent. The Kalman filter with the static steady-state model in equations 27 and 28 produces nearly identical estimates $x(t)$ as the Moving Average. Both estimators reduce the standard deviation of their estimates (σ) by approximately 50 percent (i.e., 25 percent decrease in variance σ^2) relative to the corresponding estimate from a single panel. The model in the Kalman filter ultimately reduces the estimation variance by 75 percent (1−β=1.00−0.25) in figure 7. The time-series of standardized residuals from the 2 estimators are virtually identical, with a distribution that is seemingly consistent with its expected mean of zero, unit variance, and a random temporal pattern. The standardized residuals vary between positive and negative, and they reveal no obvious non-random temporal trends. These results come as no surprise because the model in equations 27 and 28 agrees well with the true trend for this hypothetical population.

In figure 7, as in following figures, the distribution of simulated random errors from the design-based estimator for each FIA panel at time t is denoted by the red box plots and trend lines. Trend lines for the Moving Average estimator are identified in cyan, and those for the Kalman filter in green. Unlike figure 6, the box plots for error distributions from these 2 estimators are omitted to reduce clutter. Instead, their standard deviations are graphed separately. Likewise, the distributions of model prediction errors over each time step, which are portrayed with the blue box plots in figure 6, are also omitted to reduce clutter. “Saw tooth” patterns in estimated standard deviations for the Kalman filter are a consequence of model prediction errors (equation 24) that are propagated from time $t-1$ to t, immediately followed by the composite estimate (equation 21) at time t.

Relative efficiency shown in figure 7 is defined as the estimated variance of the Kalman filter estimate divided by the computed variance of the design-based estimate from the single FIA panel measured at time t. Relative variance is used as shorthand for the $1-\beta$ term in equations 19 to 21 for the Kalman filter. β represents a value between 0 and 1 that weights the design-based estimate, while the weight placed on the model-based estimate is $1-\beta$. Therefore, as $1-\beta$ nears 1, more weight is placed on the model estimate, which increases statistical efficiency attributable to the model. While there is no analogous interpretation for $1-\beta$ with the Moving Average (equation 5), it is graphed along with the $1-\beta$ for the Kalman filter as a basis for comparison. For both estimators, efficiency increases proportionally as $1-\beta$ approaches 1. The dashed line at 0.9 represents the relative efficiency expected if the sample size in the single annual panel at time t were 10–times larger, as would be the case if a periodic survey were conducted each and every year at time t.

Finally, the bottom panels in figure 7 graph the standardized residuals for the Kalman filter (equations 17 and 21). By definition, standardized residuals are expected to have a zero mean with unit variance and no temporal patterns if the model is accurate[11]. While there is no basis for this same expectation with residuals from the Moving Average (equation 4), they too are graphed along with the Kalman filter residuals for comparison.

[11] An inaccurate model can also produce residuals with the same expected distribution. Therefore, the distribution of residuals, by itself, is not a sufficient basis for a reliable test of model accuracy.

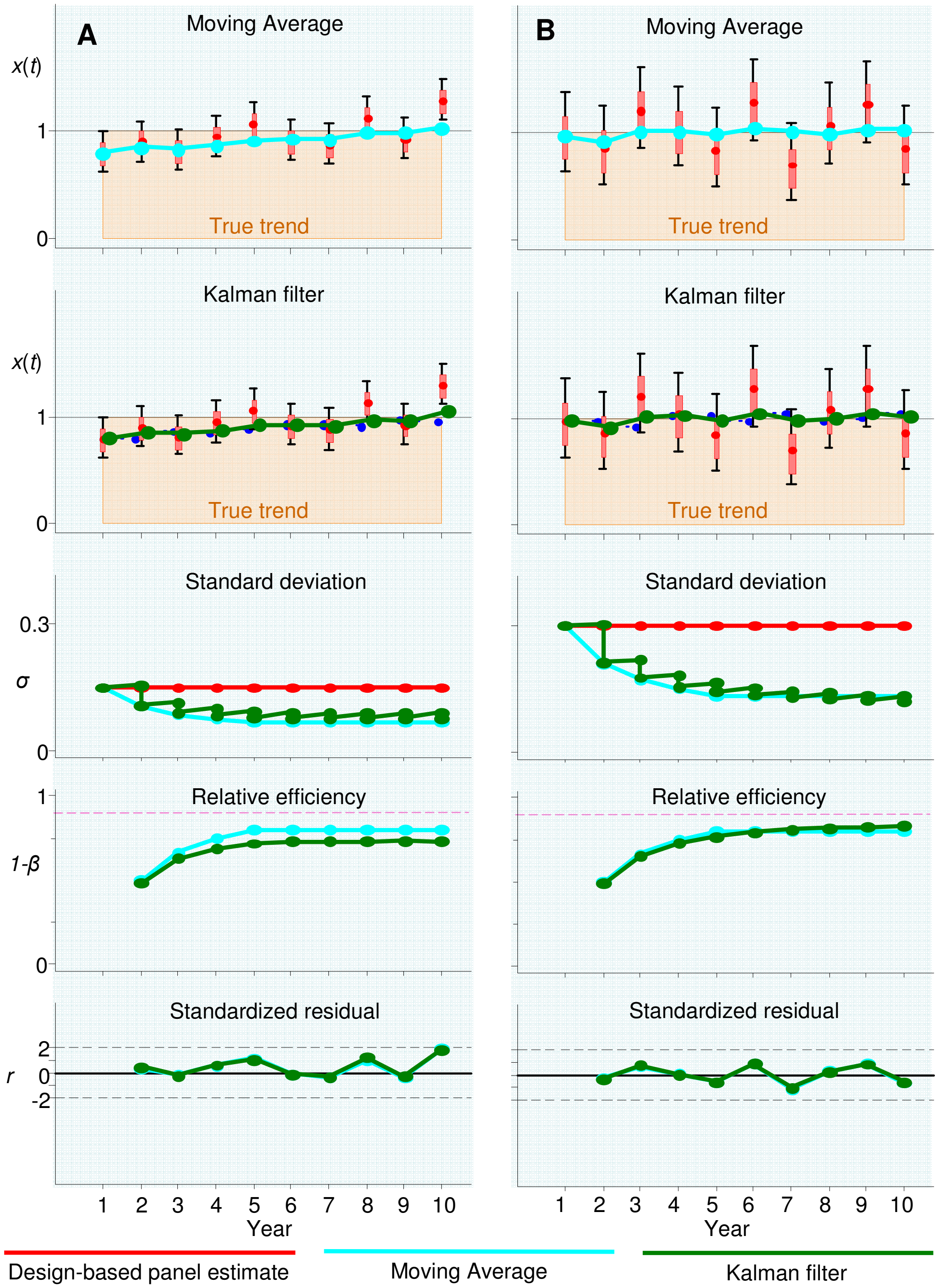

Figure 7: Comparison of Moving Average and Kalman filter estimates for a simulated population that does not change over time. The standard deviation of the estimation error is 15 percent of the population value in figure 7A (left-hand side), and 30 percent in figure 7B (right-hand side). Given these 3 realizations in the time-series of simulated sample estimates, the 2 estimators produce nearly identical results, at least in this case study of a static hypothetical population. The standardized residuals agree well with their expected values of zero mean and unit standard deviation, with no obvious trends over time in positive or negative residuals.

A second hypothetical example is given in figure 8. Unlike figure 7, this population is not static. Instead, there is an abrupt, perhaps catastrophic, 50 percent decline in the population parameter at year t=6. In figure 7A, the 5-year Moving Average exhibits "lag bias" during years 6≤t≤9, but it recovers as an unbiased estimator when the 5-year period rolls beyond the abrupt change. However, the estimated standard deviations from the Moving Average remain deceptively low, which produces seemingly very precise estimates during years 6≤t≤9, but, in reality, these same estimates are very inaccurate. On the other hand, the Kalman filter produces more accurate estimates during this anomalous time period, even though this particular implementation of the Kalman filter uses the static steady-state model. The Kalman filter estimate departs rapidly from the pre-change *status quo* at year t=6 because the Kalman filter combines the model-based estimate at year t=6 with the relatively precise estimate from the design-unbiased panel estimate at year t=6. This response is reflected by the decrease in "relative efficiency" at year t=6 as less weight is placed on the model-based estimate. However, the standardized residuals for both estimators are suspiciously extreme at year t=6, with eye-popping values of approximately −5 standard deviation units.

Figure 8B shows another estimation realization for the same simulation population. The difference being that the standardized residuals from the Kalman filter are arbitrarily (but consistently) constrained to values within ±2 standard deviations units (r_{max}=2 in equation 18). These Kalman filter estimates are remarkably accurate, especially considering that the static steady-state model is used in this particular implementation of the Kalman filter. This response to major deviations from the static model is associated with lesser weight being placed on the model-based estimates (*i.e.*, reductions in relative efficiency from the model-based estimator) and realistically larger values for the standard deviations. On the other hand, the Moving Average estimates are very inaccurate (*i.e.*, "lag bias") immediately after the abrupt change, with stunningly extreme residuals between −4.9 and −3.2 standard deviation units during years 6≤t≤8. Despite these obvious inaccuracies, the estimated standard deviations of the Moving Average estimates remain misleadingly low, which a well recognized known problem that is fully acknowledged by Patterson and Reams (2005).

Even with the constraint on the maximum standardized residual, the time-series of residuals from the Kalman filter in figure 8B exhibit an apparent temporal pattern, with consistently negative values between years 5≤t≤8. This provides weak evidence that an alternative to the static steady-state model warrants consideration, even though the Kalman filter produces reasonably accurate estimates with a misspecified model. The model-based Kalman filter can be robust even when the model is inaccurate, especially when independent design-based panel estimates are closely linked to monitoring of residuals to detect deviations from their expected distribution.

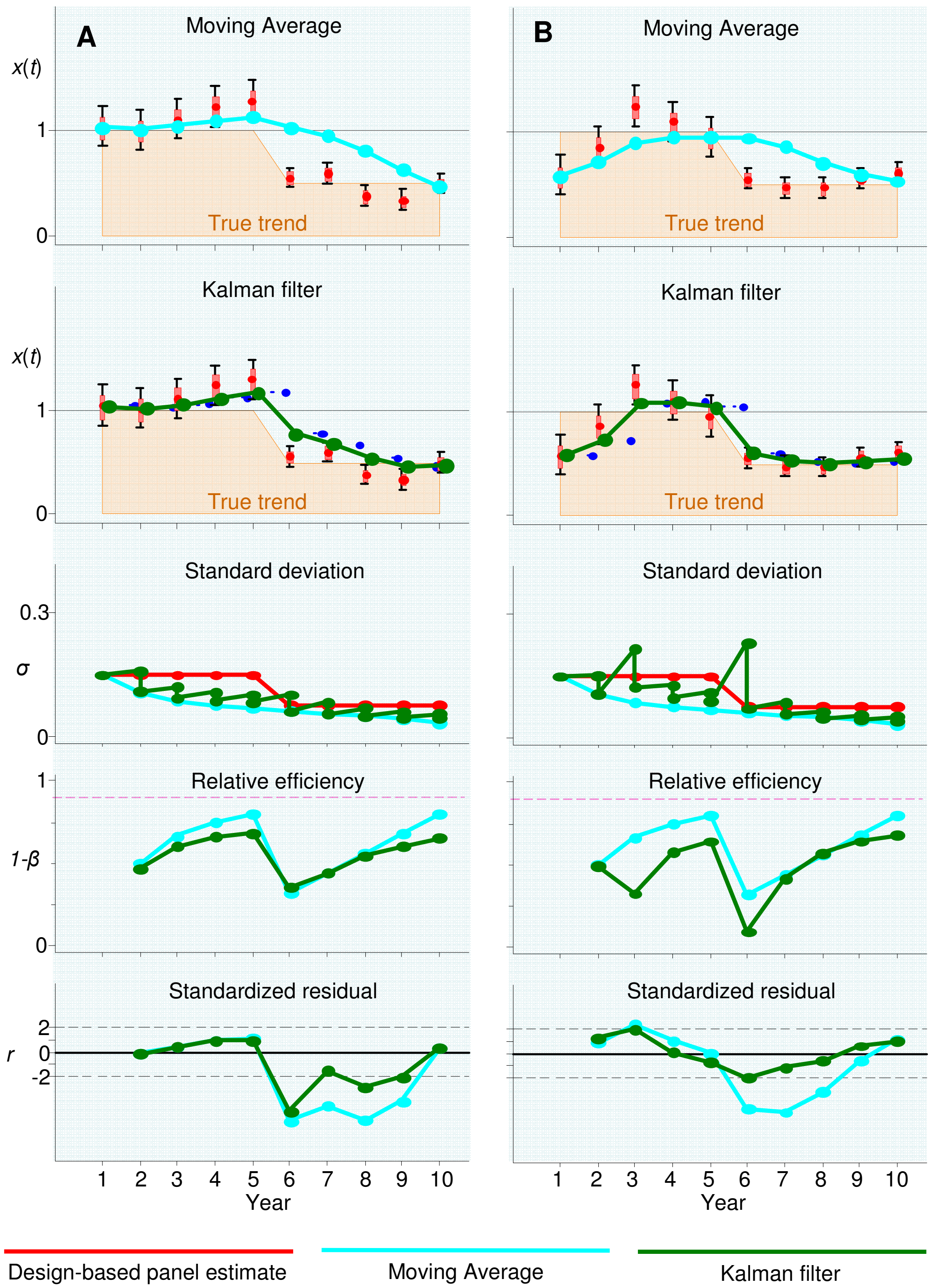

Figure 8: Comparison of Moving Average and Kalman filter estimates simulated population that changes very abruptly at year t=6. The Moving Average estimates in these 2 realizations are obviously inaccurate at year t=6 even though their estimated precisions remain relatively high. In figure 8A, both estimates exhibit improbably negative standardized residuals, although the Kalman filter is slightly better. In figure 8B, the standardized residuals for the Kalman filter are constrained to remain within r_{max}=±2 standard deviation units (equation 18). This improves the fit of the Kalman filter estimates to the true population values in this realization, but suspicious temporal trends in the standardized residuals from the Kalman filter remain.

A more problematic example is given in figure 9. As in figure 8, the population has a strong and variable pattern of change over time, while the model used in this particular implementation of the Kalman filter assumes a static steady-state. In figure 9A, the Moving Average estimates are very inaccurate, while the Kalman filter estimates are even less accurate. The standardized residuals are implausibly positive during years $2 \le t \le 6$, and curiously distributed in subsequent years. This is another example of very precise estimates that are very inaccurate. However, the results are much better in figure 9B, where same panel estimates are used, but constraints are imposed on the maximum standardized residuals for the Kalman filter (equation 18). While accuracy is not exceedingly good, the Kalman filter does produce more accurate estimates than the Moving Average, especially for years $8 \le t \le 10$. Even so, the standardized residuals from the Kalman filter exhibit strong temporal patterns, with values consistently near +2 standard deviation units during years $2 \le t \le 6$, and consistently near −2 standard deviation units during years $7 \le t \le 9$. This may be interpreted as evidence that the static steady-state model poorly represents the true temporal trends in the population. More plausible models based on independent information should be investigated.

Finally, figure 10 provides yet another example in which the population is truly changing while the model within the Kalman filter assumes a static steady-state population. The population attribute decreases 5 percent per year in figure 10A, and 10 percent per year in figure 10B. The Moving Average and Kalman filter produce nearly identical estimates. Standardized residuals from the Kalman filter are constrained by equation 18, but they are not excessive, and they reveal no obvious temporal patterns. The realized time-series of estimates and standardized residuals for the exponentially decreasing populations in figure 10 do not appear remarkably different than those for the static population in figure 7. The constraint on the Kalman filter residuals does decrease estimated efficiency relative to the Moving Average. This loss is a cost of mitigating the risk of model-based bias while preserving the potential gains from model-based efficiency with the Kalman filter. Annual panel data and estimators might not offer sufficient accuracy to detect gradual changes in a population, although even slow monotonic trends should eventually become obvious after a long time-series of panel data. However, these results should not be over-interpreted because they are merely a few realizations of sampling and estimation for several hypothetical populations.

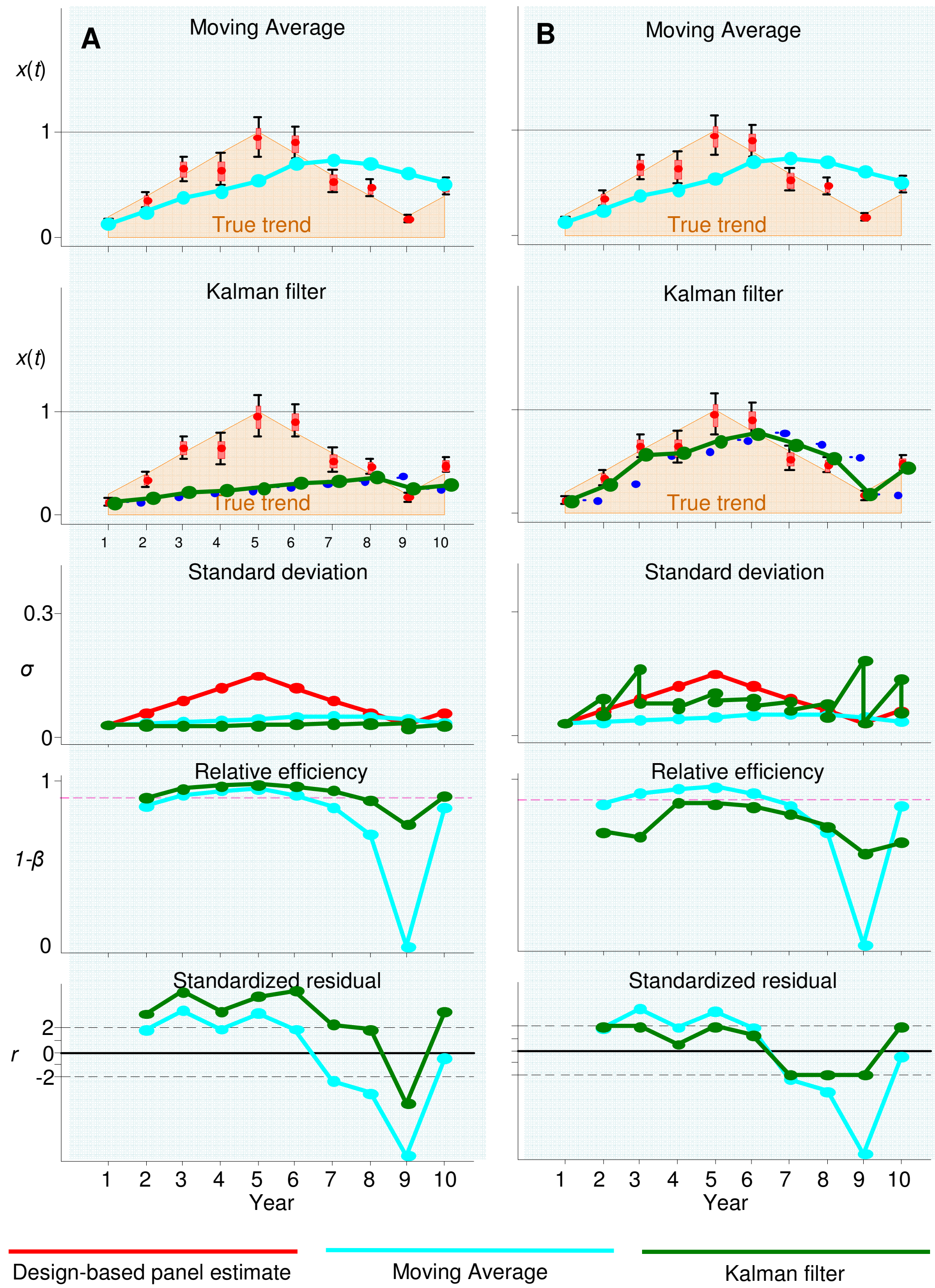

Figure 9: Both the Moving Average and the Kalman filter can appear to be very precise (i.e., low estimated standard deviation of prediction errors). However, their estimates can be very inaccurate (figure 9A). The Moving Average and the static steady-state model within the Kalman filter (equations 27 and 28) do not fit the time-series of FIA panel data very well. Constraining Kalman filter residuals to remain within $r_{max}=\pm 2$ standard deviation units improves the fit in figure 9B, even though the static model remains unchanged. However, a suspicious temporal pattern remains in the residuals (all positive for $2 \le t \le 6$ and all negative for $7 \le t \le 10$). The large residuals might indicate model misspecification rather than rare chance events. An alternative is to use independent information to select a more realistic model without the steady-state assumption.

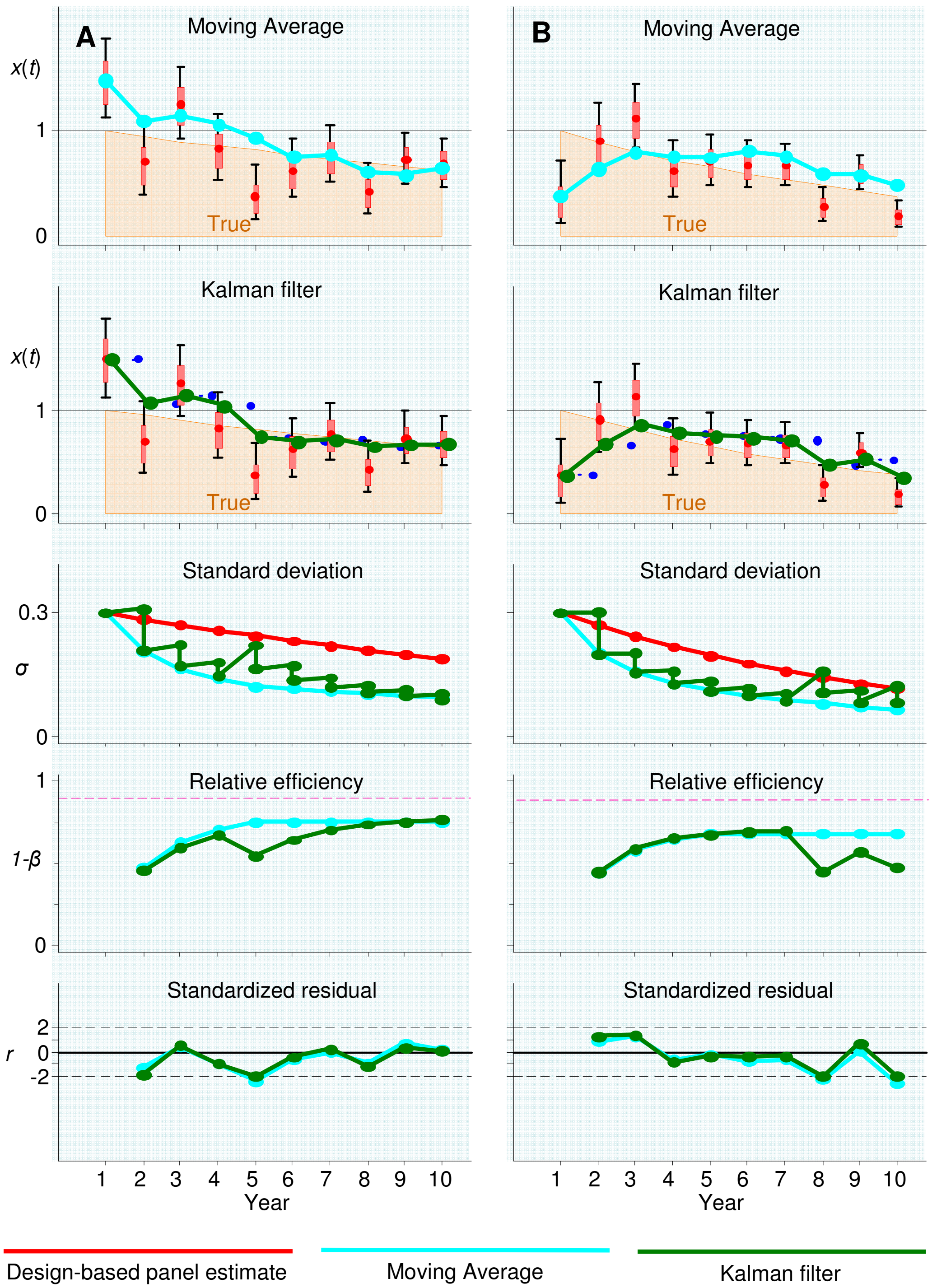

Figure 10: The Moving Average and Kalman filter can produce very similar estimates as in figure 10A, where the population is decreasing 5 percent per year and in figure 10B, where the population is decreasing 10 percent per year. There are no strong clues among the residuals that the static steady-state model (equations 27 and 28) is inaccurate. Annual design-based FIA panel data might not always be insufficient to detect true changes in a population. Constraining the Kalman filter residuals to remain within r_{max}=±2 standard deviation units (equation 18) does not notably improve the fit, although it does increase the estimated standard deviation of the predictions and reduce the efficiency offered by the model within the Kalman filter. Mitigation of risks inherent with the model-based Kalman filter (*e.g.*, equation 18) can reduce statistical efficiency.

In "real world" applications, the true population trends are unknown. Therefore, any advantages of the Kalman filter, and the relative costs and benefits from constraints on its residuals, will generally be unknown. However, these examples suggest that the Kalman filter might have desirable characteristics compared to the Moving Average. In ill-behaved situations, it appears that the model-based Kalman filter estimator can be more accurate if residuals are faithfully monitored to reveal model failures. In well-behaved situations, it appears that both estimators can yield very similar results. These preliminary impressions have not been verified with rigorous consideration of the mathematical statistics of the expected values of these 2 estimators, which is the primary tool to make generalizations about efficiency and bias (*e.g.*, Johnson and others 2003).

Monitoring Lodgepole Pine Decline in Colorado

For the last set of examples, we depart from the hypothetical and proceed to an actual time-series of annual FIA estimates. From 2002 to present, a severe epidemic of the mountain pine beetle (*Dendroctonus ponderosae*) has been devastating Colorado's lodgepole pine forests at an alarming rate. Figure 11 illustrates individual tree mortality in the foreground, and the extent of landscape-scale mortality in the background. Figure 12 maps the spread of the epidemic between 2002 and 2007[12].

The following example uses annual FIA panel estimates for Colorado to interpret the magnitude of lodgepole pine mortality caused by the mountain pine beetle outbreak. The annual FIA survey of Colorado uses 10 independent panels, each of which is a 1/10th sub-sample of all FIA field plots. The spatial distribution of sample plots within each panel is uniform over the entire state. One panel is measured in the field during each year. Each panel includes approximately 400 forested FIA field plots (table 1).

The annual FIA survey in Colorado began in 2002. There are 6 annual estimates currently available from the initial implementation of the annual FIA survey (see the first two columns in table 1). Each of the 6 design-based sample survey estimates is based on an independent sub-sample of FIA field plots (*i.e.*, a different FIA panel). However, no sample plot occurs in more than 1 panel. Therefore, the data available for monitoring state-wide trends for any single indicator of lodgepole pine condition is limited to 6 observations, namely, 1 statewide design-based panel estimate for each year.

---

12 Due to the nature of aerial surveys, the data on the maps in figure 12 will only provide rough estimates of location, intensity and the resulting trend information for agents detectable from the aerial sketchmapping surveys. The data presented on this map should only be used as a partial indicator of mountain pine beetle activity, and should be validated on the ground for actual location and casual agent. Shaded areas show locations where tree mortality or defoliation were apparent from the air. Intensity of damage is variable and not all trees in shaded areas are dead or defoliated.

Figure 11. Since 2002, the epidemic of mountain pine beetle infestations has caused catastrophic levels of lodgepole pine mortality throughout Colorado. Dead trees are shown in the foreground, and landscape-level mortality is apparent on the red slopes in the background. Image courteously of William Ciesla (U.S. Forest Service, retired).

Three indicators related to recent episodic lodgepole pine mortality are considered here: number of live trees, number of mortality trees, and number of damaged trees (table 1). The sampling distributions are assumed to be skewed because negative values are infeasible, and the distributions are assumed to be lognormal.[13] As will be seen shortly, none of the standardized residuals greatly exceeded ±2 standard deviations units; therefore, the $r_{\max}$ limit (equation 18) is not applied in this example. Unlike the hypothetical examples above, the true population trends are unknown in the these examples, but independent aerial sketchmapping (*e.g.*, Johnson and Wittwer 2006) demonstrates that the extent of lodgepole pine mortality is extensive (figure 12).

[13] A gamma distribution might also be appropriate, and future analyses should conduct goodness of fit tests to select the most representative distribution.

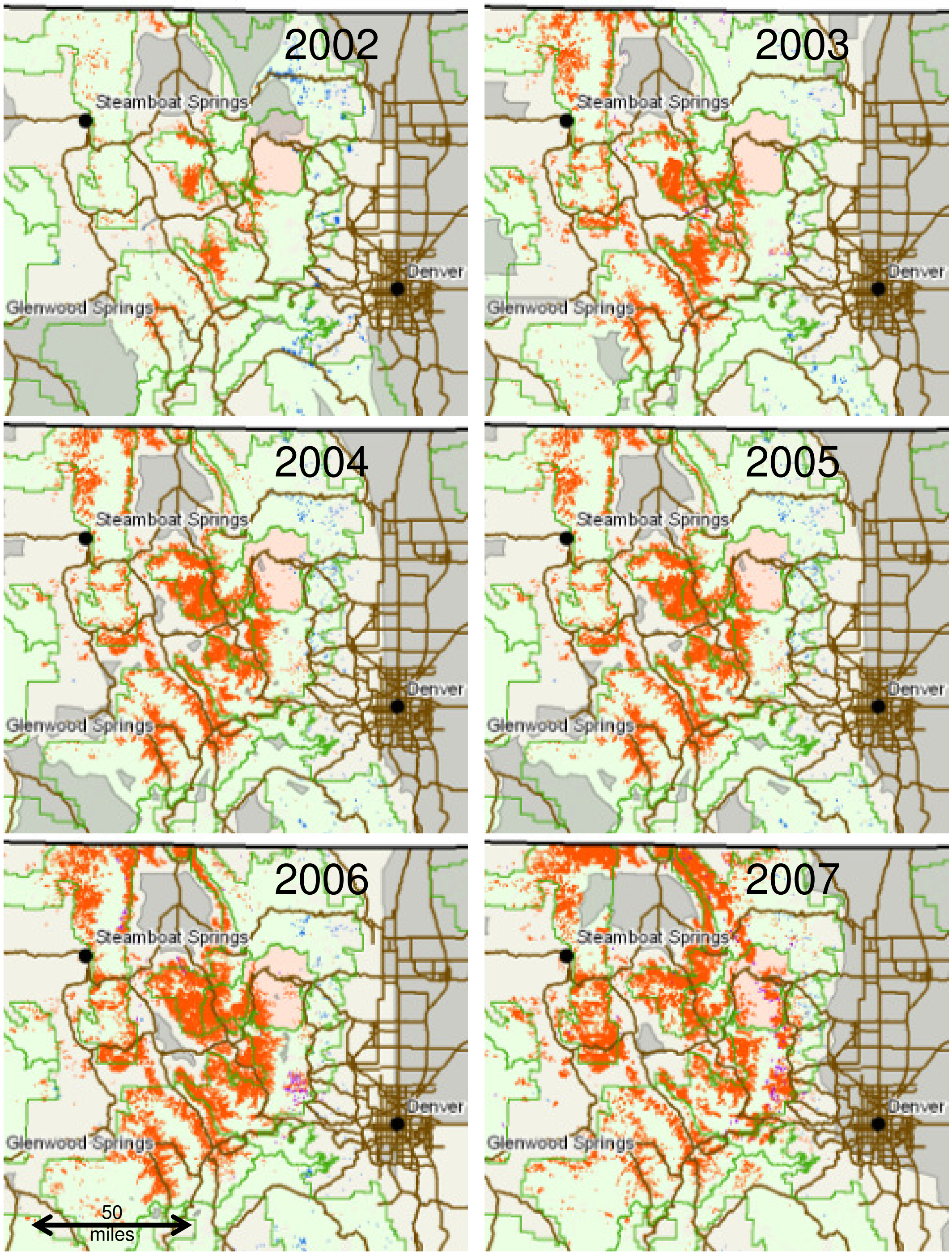

Figure 12. Epidemic spread of lodgepole pine tree mortality between 2002 and 2007 caused by mountain pine beetle in north-central Colorado[12]. The area of infestation is approximately bounded by Denver, Glenwood Springs and the border between the States of Colorado and Wyoming. Areas of heavy mortality are shaded red. These areas were identified through aerial sketchmapping (*e.g.*, Johnson and Wittwer 2006), which is a remote sensing technique that is independent of the FIA annual sample data. National Forests are shaded in green, and areas omitted from each annual survey are shaded in gray. Cartographic products were provided by Jennifer Ross (U.S. Forest Service, Rocky Mountain Region, Forest Health Management Service Center, Lakewood, CO).

Table 1: Lodgepole pine statewide estimates for Colorado from 6 annual FIA panels. These are include all sufficient statistics necessary to apply the Moving Average and Kalman filter estimators in figure 13 to figure 15.

Design-based estimator			**Model-based time-series estimators using annual FIA panels**								
Annual FIA panels[a]			**Moving Average**[b]				**Kalman filter**[c]				
Year	**Estimated mean**	**Standard deviation of estimate**	**Estimated mean**	**Standard deviation of estimate**	**Standardized residual**[d]	**Relative efficiency**[e]	**Estimated mean**	**Standard deviation of estimate**	**Relative efficiency**[f]	**Standardized residual**[g]	**Number of forested plots in annual panel**
Average number of live trees per forested acre[h]											
2002	26.30	4.50	26.30	4.50			26.30	4.50			362
2003	27.47	4.25	26.89	3.10	0.13	0.47	26.94	3.15	0.45	0.18	387
2004	36.48	6.17	30.08	2.91	1.14	0.78	29.18	2.99	0.77	1.35	409
2005	28.79	4.91	29.76	2.51	-0.21	0.74	29.06	2.73	0.69	-0.06	407
2006	20.13	3.48	27.83	2.12	-2.25	0.63	25.12	2.31	0.56	-1.92	391
2007	20.49	4.14	26.67	2.09	-1.61	0.74	23.72	2.28	0.70	-0.93	411
Average annual number of mortality trees per forested acre averaged over 5-year period[i,j]											
2002	0.10	0.06	0.10	0.06			0.10	0.06			362
2003	0.09	0.03	0.10	0.03	-0.06	0.05	0.10	0.03	0.13	-0.56	387
2004	0.16	0.07	0.12	0.03	0.67	0.78	0.15	0.05	0.54	0.06	409
2005	0.13	0.05	0.12	0.03	0.26	0.73	0.16	0.04	0.31	-1.05	407
2006	0.31	0.12	0.16	0.03	1.47	0.93	0.27	0.07	0.67	0.42	391
2007	0.63	0.24	0.26	0.06	1.85	0.94	0.44	0.11	0.80	0.84	411
Average number of live trees per forested acre damaged by insects[k,i,l]											
2002	0.20	0.10	0.20	0.10			0.20	0.10			362
2003	0.67	0.41	0.44	0.21	0.63	0.74	0.35	0.14	0.88	0.86	387
2004	1.17	0.57	0.68	0.23	0.98	0.83	0.61	0.21	0.86	1.07	409
2005	0.46	0.19	0.63	0.18	-0.71	0.08	0.57	0.17	0.24	-1.16	407
2006	1.88	0.71	0.88	0.20	1.71	0.92	1.04	0.31	0.81	1.31	391
2007	2.11	0.90	1.26	0.27	1.14	0.91	1.69	0.44	0.76	0.54	411

[a] These design-based FIA panel estimates (Scott and others 2005) are sole sufficient statistics used to apply the Moving Average and Kalman filter.

[b] Moving Average defined in Equations 1 and 2.

[c] Univariate Kalman filter defined in equations 19 to 24.

[d] The standardized residual for the Moving Average (r_{MA}) is defined in equation 4.

[e] Relative efficiency (1-β) is defined for the Moving Average in equation 5.

[f] The relative efficiency for the Kalman filter is defined with equation 21.

[g] The standardized residual for the Kalman filter is defined in equation 17.

[h] Kalman filter estimates for total live lodgepole pine tree use the static model with low prediction error (equations 27 and 28, graphed in figure 13).

[i] Kalman filter estimates for lodgepole pine mortality and damage use exponentially increasing model with moderate prediction error (equations 25 and 26).

[j] Graphed in figure 14C.

[k] Graphed in figure 15C.

[l] Tree damage estimates are the basis for examples in figure 5 (2002 only) and figure 6 (2002 to 2007).

Total Numbers of Live Trees

The estimated total numbers of live lodgepole pine trees in Colorado for each year are graphed in figure 13 on page 35. The graph symbolism remains the same as that described on page 20. The initial analysis of this indicator with the Kalman filter used the static steady-state model in equations 27 and 28, which resembles a null hypothesis in which there is zero net change over time.

Both the Moving Average (equations 1 and 2) and the Kalman filter produce very similar time-series estimates (figure 13, table 1). After the initial few years of relatively scant panel data, the variances of the annual estimates average about 33 percent of those for the design-based estimates from each panel, meaning the time-series of Moving Average and Kalman filter estimates have about the same precision as a single sub-sample with 3-times the number of field plots.

The downward trending design-based panel estimates in figure 13 are consistent with the mountain pine beetle epidemic in Colorado. However, the static steady-state model in the Kalman filter fits these data reasonably well. There is nothing obviously askew with the magnitude and temporal trends in the standardized residuals. However, it is very possible that an alternative model would better fit the annual panel estimates, although this possibility was not investigated here.

Tree Mortality

The annual panel estimates for 2006 and 2007 suggest an increasing mortality rate in figure 14 on page 36. However, the spread of the design-based estimation error for any single panel is somewhat broad relative to the apparent trend. Recall from page 20 that the red box plots in figure 14A mark the 10^{th}, 25^{th}, 50^{th}, 75^{th} and 90^{th} percentiles of the assumed lognormal distribution with the first 2 moments estimated from the panel data each year. There is a small but plausible chance that the panel estimates in 2006 and 2007 could have been observed even if mortality did not increase beyond the levels in 2002 to 2005. However, the standardized Kalman filter residuals in 2006 and 2007 are suspiciously large (standard deviation units of 1.55 and 2.08 respectively). Under the steady-state model assumed in this case for the Kalman filter, and assuming an expected normal distribution of residuals with zero mean and unit variance, the individual probabilities of each standardized residual are 6 percent and 2 percent respectively. However, had there been an *a priori* hypothesis that the panel estimates would have shown unusually high mortality rates in 2006 and 2007, the single-tailed joint probability of both events would have been $(0.06/2) \times (0.02/2)$, or roughly 0.02 percent. That joint probability is unlikely given the steady-state model and other assumptions.

One alternative hypothesis retains the assumption that the population variable is at a static steady-state (*i.e.*, φ=1 in equation 22), but assumes the annual prediction error is very high instead of very low, which would be characteristic of a dynamic population with annual perturbations that range widely around a constant level. Based on professional judgment, and independent of the observed annual panel estimates, assume a coefficient of variation of 1.00 for the random prediction errors over 1 year prediction interval. Recall that the previous model assumed a coefficient of variation of 0.05. The result is the exact same model for the population variable as equation 27 and figure 14A, but replacing the variance propagation model in equation 28 with:

$$\sigma_x^2(t|t-1) = \sigma_x^2(t-1|t-1) + [1.00 \times x(t-1|t-1)]^2$$

[29]

The outcome is given in figure 14B. The Kalman filter fits the 2006 and 2007 panel estimates notably better than under the model used for figure 14A. They also fit better than the Moving Average estimates. Furthermore, the time-series of 6 standardized residuals with the modified model does not reveal as strong of an apparently non-random temporal pattern. While the estimated precision from the Kalman filter decreases, the predictions are more plausible given the design-based panel estimates. Unfortunately, the precision with the Kalman filter is not much better than that with the annual FIA panel estimates before the mountain pine beetle epidemic. The model used by this particular Kalman filter contributes little to increased statistical efficiency, at during early stages of the beetle outbreak, and the gain is only marginal thereafter. Most of the information derives from the annual design-based panel estimates, and very little information is gained from model predictions based on past panels.

A third hypothesis is that lodgepole pine mortality is increasing during the beetle epidemic. Based on independent observations, for example forest health reconnaissance with aerial sketchmapping (figure 12) and expert judgment, assume an exponentially increasing model for lodgepole pine mortality between 2002 and 2007, where the mortality rate increases 50 percent (1.5 times) per year, with a coefficient of variation for the random prediction errors over 1-year of 0.25 (*i.e.,* a standard deviation equal to 25 percent the magnitude of the number of mortality trees). This is the same model as that defined in equations 25 and 26 and used to build figure 6, which provides a more detailed example of how the Kalman filter works.

The results for the Kalman filter with the exponentially increasing model from equations 25 and 26 are given in figure 14C and table 1. The fit to the annual design-based panel estimates improves to a modest degree, and surpasses that from the Moving Average. The relative efficiency is intermediate between that from the unrealistic static model (figure 14A) and the uninformative static model (figure 14B). The 6 standardized residuals more resemble their expected distribution, which has zero mean and unit variance, and their temporal pattern appears more random. However, strong inference regarding the distribution of standardized residuals is rarely possible with only 6 observations.

The model coefficients used in this example are based on expert judgment, and they are not empirically fit to FIA panel data. This process of model parameterization preserves the scientific process in hypotheses formulation and avoids “data mining.” With small datasets, there is a risk of misinterpreting a pattern that is caused, in reality, by random processes. For example, sampling error with a small number of annual panel estimates can cause apparent temporal trends in a population that is truly at a static steady-state (e.g., figure 7A and the first 5 years in figure 8). Data mining has a more valid role in the analysis of much larger datasets, where this risk can be less.

This example helps illustrate that no single model or estimator is necessarily “correct.” However, there can be a difference when trying to interpret the trends. The Moving Average fits the data (figure 14A), but how does that help answer important analysis questions regarding tree mortality? The static model fits the data when the uncertainty of model predictions is assumed high (figure 14B), but how does that offer any more insights than the Moving Average? The exponentially increasing model also fits the data (figure 14C and table 1), perhaps somewhat better than the alternative hypotheses. However, this final hypothesis suggests that tree mortality measured at time t is about 1.5 times that measured at time t-1, which is an increase of about 50 percent per year. This provides a more meaningful interpretation of the trend data than the alternative models (hypotheses) considered here. If a model is not a meaningful representation of the scientific hypothesis of interest, then “everything is compromised” (Anderson 2008).

Tree Damage

FIA field crews assess damage and insect or pathogen activity that seriously affects live trees with diameter at breast height ≥5.0 inches (U.S. Forest Service 2007b). Based on judgment of the field crew, such damage will likely prevent the tree from living to maturity, or surviving 10 more years, if already mature; or the damage will likely reduce the quality of the tree’s products (e.g., potentially resulting from lightning strike, excessive lean, tree rot). Whenever feasible, field crews subdivide insect damage into more specific agents, including mountain pine beetles, bark beetles, defoliators, terminal weevils, and *Ips* engraver beetles.

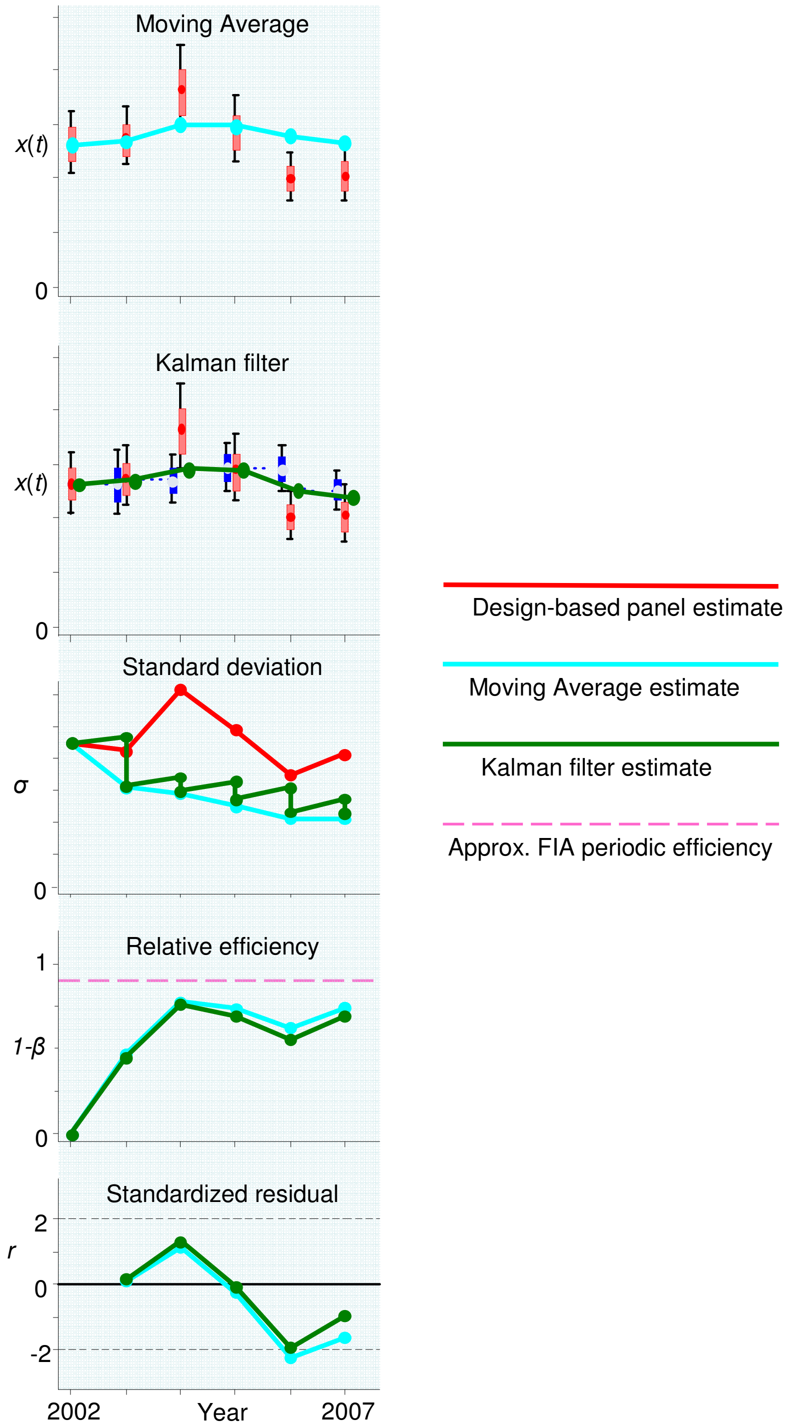

Figure 13: Estimated total number of lodgepole pine trees in Colorado from 2002 to 2007 using independent annual FIA panels. These are actual design-based FIA estimates (Scott and others 2005), and the true population trend is unknown. Both the Moving Average and the Kalman filter yield very similar annual estimates. There is no strong indication from the standardized residuals that the static steady-state model in the Kalman filter (equations 27 and 28) is inaccurate. If there is a true change in the number of lodgepole pine trees in Colorado between 2002 and 2007, then the observed data and the chosen estimators are not powerful enough to detect the change. This figure is discussed on page 32.

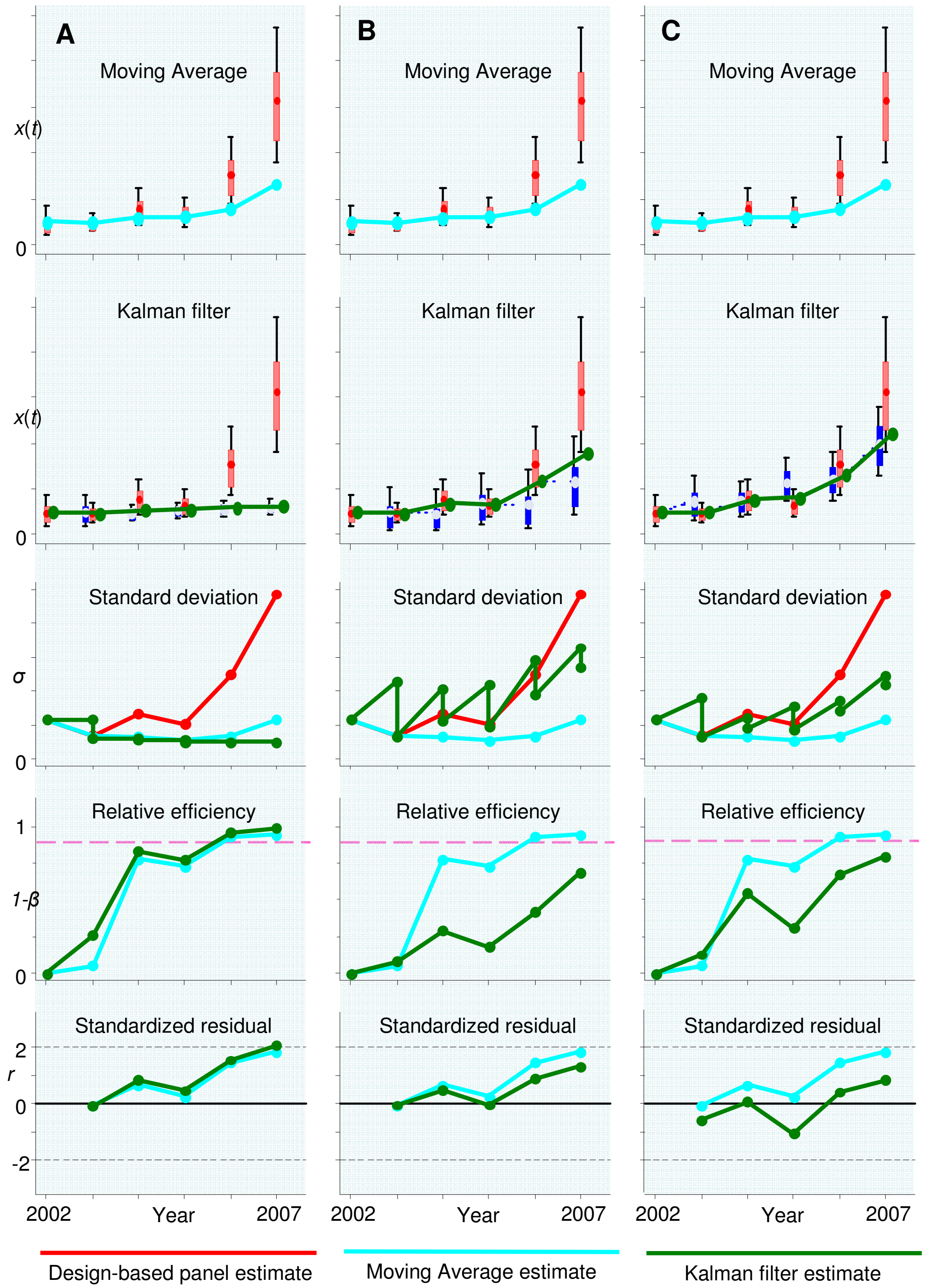

Figure 14: Estimated lodgepole pine tree mortality in Colorado. The Kalman filter with the static steady-state model (equations 27 and 28) does not accurately fit the annual FIA panel estimates in 2006 and 2007 (figure 14A). The fit in figure 14B improves assuming a static model with a much larger random forecasting error (equations 27 and 29). A similar fit in figure 14C is achieved assuming an exponential rate of increase with a moderate degree of forecasting error (equations 25 and 26). The exponentially increasing model has somewhat more plausible residuals. More importantly, it provides the most useful interpretation of the trend in the panel data, which is consistent with the epidemic of pine beetle mortality that is obvious across Colorado. This figure is discussed on page 32.

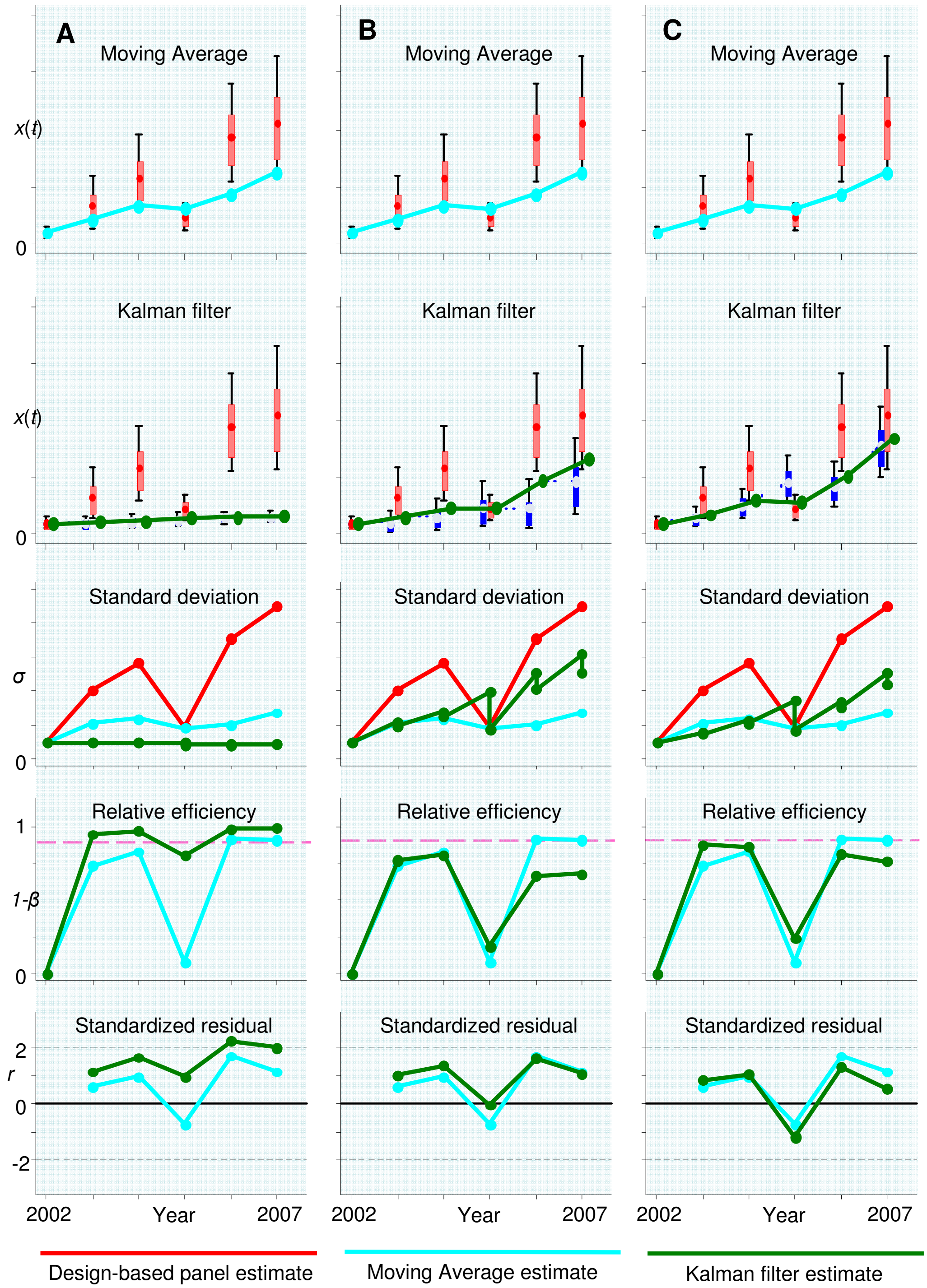

Figure 15: Estimated tree damage in Colorado. Results are very similar to those for tree mortality in figure 14, and the same models are used in figure 15. A multivariate Kalman filter could be formulated that simultaneously predicts total number of trees, tree mortality and tree damage. A multivariate population dynamics model in the Kalman filter might account for the expected biological processes during a pine beetle epidemic. This might improve the accuracy of the time-series estimates and the power to differentiate among alternative models within the Kalman filter. This figure is discussed on page 34.

The estimated time-series of mountain pine beetles damage to live lodgepole pine trees in Colorado is given in figure 15 on the previous page. The results are qualitatively very similar to those for tree mortality. The precise static model (equations 27 and 28) poorly fits the annual FIA panel estimates in figure 15A, while the imprecise static model (equations 27 and 29) fits about as well as the Moving Average (figure 15B), but the model does not markedly help improve statistical efficiency. On the other hand, the exponentially increasing model in equations 25 and 26 fits slightly better (figure 15C and table 1). More importantly, interpretation of the exponentially increasing model in terms of the beetle outbreak is more useful for analyses than the Moving Average and Kalman filter with an imprecise steady-state model.

Discussion

The exposition and examples given above are primarily intended to introduce the reader to the Kalman filter and its relevance to FIA strategic goals and objectives for annual monitoring (U.S. Forest Service 2007a). We hope this helps every reader understand the Kalman filter, at least in an intuitive sense, while providing sufficient, yet simple, mathematical details to serve as an introduction to statisticians. The remaining few sections touch upon more technical issues that warrant future study by FIA analysts and statisticians. The purpose is to suggest possible approaches to improve statistical accuracy, analyses of residuals, quantitative comparisons of alternative hypotheses and statistical estimators, and implementation within FIA information management systems.

Analyzing Trends with Annual FIA Data

Three immediate questions arise when temporal trends are interpreted with annual FIA panel data:

1. From a simple graphical display, is there an observable trend in population parameters over time?
2. If so, does the trend make sense? For example, increased mortality would be expected as the result of a known catastrophic disturbance event, such as bark beetle outbreaks, severe weather, *etc*.
3. Is the trend significant relative to the uncertainty in the population estimates?

For lodgepole pine mortality in Colorado caused by mountain pine beetle, the answer seems to be “yes” for all three questions. The third question has been addressed in previous studies[14] with analysis of variance and regression. A simple statistical regression with annual panel data verifies there is a significant upward trend in mortality and damage between 2002 and 2007. Analysis of variance identified two combinations of panels that were significantly different from each other. But can the Kalman filter add value beyond the more traditional approaches?

The analyses with the Kalman filter can estimate the temporal trend in tree mortality and damage. Although the Moving Average and regression can accomplish this same task, the results from the Kalman filter may be more interpretable. Furthermore, the Kalman filter can fit the annual panel estimates more accurately. This addresses the first and second questions.

The Kalman filter weights each annual FIA panel estimates with a ratio of variances, which intuitively makes sense and is easy to understand. The Kalman filter can accommodate quantitative models that are based on theory, and alternative models can compare alternative theories and their relative fit to empirical data. This also addresses the second question.

The Kalman filter can compare alternative models with the static steady state model, which resembles a null hypothesis in analysis of variance and regression analyses. This addresses the third question. However, more meaningful hypotheses, in the form of annual transition models (*e.g.*, φ_t in equation 22), may be captured within the Kalman filter. In this context, ranking of alternative hypotheses is discussed in the next section.

Selecting Among Alternative Hypotheses and Estimators

The analyses illustrated in figures 7 to 10 and 13 to 15 employ two different time-series estimators: the Moving Average and the Kalman filter. In addition, the Kalman filter employs intrinsically different temporal models for a population parameter (e.g., static steady state v. exponentially increasing state).

If the Moving Average is used as an unbiased estimator of the current population parameter, then a static or steady-state model is likely implied, in which there is no net change in the population over time. If the Moving Average is assumed to be the minimum variance estimator, then this likely implies temporal homoscadasticity of sampling and prediction errors.

The Kalman filter model used in some of the above analyses shares the same steady-state model with the Moving Average estimator, although the Kalman filter utilizes additional assumptions about the magnitude of time-invariant model prediction errors. Steady-state equations 27 and 28, which are the basis for figure 7 to 13, 14A and 15A, assume a temporally indifferent distribution of random

[14] M.T. Thompson, in review, *Western Journal of Applied Forestry.*

prediction errors with a relatively small standard deviation of annual prediction error (i.e., 5 percent coefficient of variation). Steady-state equations 27 and 29, which are used for figure 14B and figure 15B, assume much more variable annual prediction errors (i.e., 100 percent coefficient of variation). The models used in the Kalman filter analyses for figure 14C and figure 15C, which are defined with equations 25 and 26, hypothesize an exponentially increasing rate of 50 percent per year with modest variability in random annual prediction errors (i.e., 25 percent coefficient of variation).

Which Kalman filter model best fits the annual FIA panel estimates? Is the Kalman filter a more precise estimator than the Moving Average? These questions may be conditionally answered if simplifying assumptions and models are correct. Unfortunately, assumptions and models are virtually always incorrect to varying and unknown degrees. Figure 8A and figure 9A are obvious examples, where it is assumed that prediction error is low because the model is very accurate. Apparently, this assumption is exceedingly overoptimistic because the standardized residuals are suspiciously large[15], with values ranging between -6 and -8 standard deviation units during certain time periods.

The *ad hoc* rule in equation 18 increases the estimate of model prediction error variance based on the analysis of residuals. This rule assures that the residual difference between the model-based prediction and the design-based panel estimate never exceeds 2 standard deviation units, which makes this rule an integral (non-linear) part of the model for prediction errors within the Kalman filter. This rule improves the agreement between the Kalman filter estimates and the true population trends in the hypothetical examples, which is illustrated in figure 8B and figure 9B. But the true trend is never known in actual applications, and this rule was not invoked in the example of annual FIA data for lodgepole pine mortality in Colorado (figures 13 to 15).

Again, how do we select the best hypothesis and estimator among a set of alternatives? Anderson (2008) provides a particularly useful view of comparisons among competing hypothesis and models. This view might help guide analyses of residuals from alternative estimators and models. The following section uses heuristics to briefly explore this train of thought. However, these comments are intended merely to invoke further investigation, and not as a prescription for data analysis.

Entropy and Information-Theoretics: Van Deusen (1999) suggests that alterative hypotheses regarding polynomial temporal trends within the mixed estimator may be compared with the Akaike information criterion (AIC) of Akaike (1974) or the Schwarz information criterion (SIC) of Schwarz (1978)[16]. Burnham and Anderson (2001) review a closely related method from information-theoretics that ranks the fit of alternative models to representative observations,

---

15 Deceivingly implausible residuals are possible when the model is accurate, at least in rare cases.

16 Van Deusen (1999) recommends the Schwarz information criterion in his setting.

where the models represent alternative hypotheses and the fit is measured by observable residuals.

As an embellishment to the likelihood perspective, Burnham and Anderson (2001) describe an AIC method based on residual statistics that are assumed to be normally distributed. This method might be applicable to residuals from the Moving Average (equation 3) and the Kalman filter (equations 15 to 17). If it is applicable, then this method would allow ranking among models (i.e., hypotheses) based on the Moving Average, the steady-state Kalman filter with low prediction error (equations 27 and 28), the steady-state Kalman filter with high prediction error (equations 27 and 29), and the exponentially increasing Kalman filter with moderate prediction error (equations 25 and 26).

The relevant AIC statistic is given by Burnham and Anderson (2001, 2004) as

$$\begin{aligned}
&\mathrm{AIC} = n \log\left(\hat{\sigma}_\varepsilon\right) + 2K \\
&\text{where} \quad \hat{\sigma}_\varepsilon = \sqrt{\frac{\sum \varepsilon_i}{n}} \\
&\varepsilon_i = \text{residual difference between model and data at point } i \\
&n = \text{number of residuals} \\
&K = \text{number of estimated model parameters}
\end{aligned} \qquad [30]$$

Now consider the afore mentioned heuristics. Let the residuals from the Moving Average estimator be defined as r_{MA} in equation 4, and residuals from the Kalman filter as $r(t_2)$ in equation 15. If each residual were divided by its estimated standard deviation from the design-based panel estimator, then perhaps one might approximate equation 30 with[17]:

$$\begin{aligned}
\hat{\sigma}_\varepsilon &= \sqrt{\frac{\sum_{i=2}^{P}\left[r_{MA,i}^2 \big/ \sigma_{z_i}^2\right]}{P-1}} \quad \text{for the Moving Average} \\
\hat{\sigma}_\varepsilon &= \sqrt{\frac{\sum_{i=2}^{P}\left[r\left(t_{i|i=1,\cdots,P}\right)^2 \big/ \sigma_{z_i}^2\right]}{P-1}} \quad \text{for the Kalman filter}
\end{aligned} \qquad [31]$$

Multivariate vector residuals may be similarly normalized through matrix multiplication by the inverse Cholesky square root of the covariance matrix for estimation errors from the design-based annual panel estimates. Under the

17 Residuals are not available at the time of initial conditions (t=1).

assumption of negligible model bias and adequate estimation precision, residuals so normalized may be treated as orthogonal with unit variance, and summed together under the assumption that they where all independent and identically distributed. Simultaneous analyses of orthogonal multivariate residuals would provide more observations and stronger evidence when comparing alternative hypotheses and univariate estimators.

Burnham and Anderson (2001) state that the "*AIC* (equation 30) *is not a test in any sense: no single hypothesis (model) is made to be the 'null', there is no arbitrary α level, and there is no arbitrary notion of 'significance'. Instead, there are concepts of evidence and a 'best' inference, given the data and the set of* a priori *models representing the scientific hypotheses of interest. … Akaike's general approach allows the best model in the set to be identified, but also allows the rest of the models to be easily ranked*."

Burnham and Anderson's ranking method only considers hypotheses that are identified explicitly during the analysis. There is no guarantee that some other hypothesis, which was not considered during the analysis, is a better fit to the observed data. For example, the static steady state model in equations 23 and 24 for total number of live lodgepole pine trees provides a reasonable fit the annual FIA panel estimates (figure 13). This model is much like a null hypothesis. However, there is independent evidence from aerial sketchmapping that strongly suggests that the number of live trees should be decreasing (figure 12), not static. An alternative model that predicts a decline in the number of live trees might fit the panel data better that the static model, but the model that predicts a decline was not included in this particular analysis. This is an example of an undesirable omission.

The examples of indictors of lodgepole pine demographics demonstrate the potential inadequacy of tests for a null hypothesis of no change. The null hypothesis may fail to be rejected based on the available data, even when some other hypothesis may have better fit the same data. Therefore, any meaningful analysis should include a set of reasonable *a priori* alternative hypotheses that can be ranked relative to their agreement with independent observations. However, inclusion of a model that mimics a null hypothesis, such as the static steady state model in equations 23 and 24, can provide a relative "baseline" when comparing the differences among AIC statistics for alternative hypotheses. For example, compare 3 models (hypotheses) that predict a percent per year decline in live trees of 25, 50 and 75 percent. The AIC statistics in this hypothetical example are given in table 2. Is the difference in their AIC statistics relatively large or relatively small? Comparisons of these AIC statistics relative to the AIC statistic for the static model (i.e., no annual change) can help answer this question.

In the absence of a model that assumes a static steady state, the AIC statistics in table 2 seem to strongly highlight the model with a 50 percent annual rate of change because the relative AIC for that model is high relative to the other alternatives (25 and 75 percent per year change). However, the differences among dynamic models (25, 50 and 75 percent per year) are less striking when the static steady state model (0 percent annual change) is used as the baseline[18] The latter comparisons suggest that there is a decline in number of live trees, as would be expected, but there is not strong evidence for estimating the actual rate of change (25, 50 or 75 percent per year).

Table 2 Hypothetical ranking of alternative hypotheses for annual rate of change with the AIC statistic (equations 30 and 31).

Change rate per year	No static model		Static model included[18]	
	AIC	Difference	AIC	Difference
0%			10,000	0
25%	10,200	0	10,200	200
50%	10,250	50	10,250	250
75%	10,225	25	10,225	225

Multivariate Kalman Filters

Multivariate versions of the Kalman filter can improve the accuracy and reliability of time-series estimates, and accommodate more realistic models of ecosystem processes. Some of these issues are briefly covered in this section. Though the complexity of a multivariate approach can be initially intimidating, the basic concepts behind complex Kalman filters are just as simple as the univariate version considered above.

Complex Tree- and Stand-level Models: Tree damage is a leading indicator of tree mortality, and tree mortality is negatively correlated with the number of live trees. This suggests a multi-response model in the Kalman filter that simultaneously considers the demographics of the statewide lodgepole pine tree population, where the average number of trees per forested acre at time t equals the tree density at $t-1$, plus the average number of ingrowth trees and minus the average numbers of new mortality and removal trees per acre between $t-1$ and t.

More accurate and detailed model predictions may be available from deterministic growth and yield models. In principle, any deterministic population or ecosystem model can be linked to the Kalman filter to improve estimates and the analysis of broad-scale trends (e.g., Van Den Brakel and Visser 1996, Williams and others 2005, and Tian and Xie 2008). Multivariate predictions from a complex nonlinear model can be made for each FIA plot or tally tree, using the most recent field measurements as initial conditions. Examples include the Forest Vegetation Simulator (Crookston and Dixon 2005, Miles 2008) and models fit to

[18] Recall that the static model for live trees fit the annual FIA panel data reasonably well in figure 13

FIA plot data by Lessard and others (2001) for updating annual forest surveys. Imputation can be viewed as an empirical multivariate prediction model, which has already been applied in the context of annual FIA surveys (Van Deusen 1997, Reams and McCollum 2000, McRoberts 2001, Gartner and Reams 2002, and Eskelson and others 2008). However, if alternative hypotheses will be compared during analysis, then deterministic models, such as the Forest Vegetation Simulator, should be used rather than purely empirical methods, such as imputation. Deterministic models can capture assumptions about future population dynamics, whereas purely empirical methods use past observations to predict future conditions.

Imputations or predictions from the model for each tree or FIA sample plot can be used to estimate the predicted state vector at the population level. This is accomplished with design-based sample survey methods, exactly like those used with actual field measurements. Those multivariate sample survey estimates are then assimilated into the Kalman filter through a multivariate transition matrix, which is analogous to the univariate φ_t in equations 23 and 24. One challenge would be estimation of the covariance matrix that describe model predictions error, analogous to the scalar variance $\sigma_w^2(t)$ in equation 24 plus any quantified estimation error associated with the transition matrix (Ni and Zhang 2008).

Such models could be formulated to compare alternative hypotheses that are related to forest health. The Forest Vegetation Simulator can model effects of disturbance agents, including insects, pathogens, and fire (Crookston and Dixon 2005). Hypotheses may be based on climate change scenarios, the consequences of which are modeled with the Forest Vegetation Simulator (*e.g.,* Malmstrom and Raffa 2000; Crookston and others 2008). Hypotheses may be formulated with a demographic model that predicts the spatial dynamics of a pest population and the associated damage to trees (*e.g.,* Logan and others 2003). Ranking the degree of agreement between model predictions and direct observations, such as annual FIA panel estimates, is briefly covered on page 39.

Standardization of Multivariate Vector Residuals: If all assumptions incorporated into a Kalman filter are approximately correct, then the standardized residuals should be approximately distributed with a zero mean, unit variance, and mutual independence over time (Maybeck 1979). If there is a convincing deviation of the standardized residuals from their expected distributions, then there is evidence of model misspecification. It can not be overemphasized that close scrutiny of residuals is essential to mitigate the risk from a model-based approach, such as the Kalman filter, while preserving the gains in efficiency that are possible with the model-based approach.

In a large and complex governmental statistical system like FIA, this level of scrutiny would have to match that already conducted to detect other sorts of non-sampling errors (*e.g.,* Pollard and others 2006). FIA database software could be augmented with a hypothesis test that the set of standardized residuals from recent FIA panels and annual estimates fits a normal distribution with mean zero and unit variance; the Kolmogorov-Smirnov test is an example. The database could include a test that the time-series of recent residuals from the composite estimator in the Kalman filter fulfill the expectation of mutual independence over time; the non-parametric Wald-Wolfowitz runs test is an example.

If population-level estimates from the deterministic models demonstrate a good fit to the time-series of FIA panel estimates, and analyses of residuals reveal no suspicious deviations from expectations, then the accuracy of the statistical estimates with the Kalman filter will likely improve. If the fit is mediocre, at least the Kalman filter is robust against modest levels of model misspecification. Furthermore, any lack of fit, assuming it is actually discovered during an analysis, provides the opportunity to learn more about the system and improve the models. Monitoring and analysis of vector residuals from the Kalman filter could assist in this learning process.

Remotely Sensed Data: Ancillary remotely sensed data can improve the estimated area of forest, including separation of estimates into forest area with and without severe insect damage (e.g., Wulder and others 2005 2006a 2006b, Goodwin 2008). The Kalman filter can combine multi-response process models for land use, land cover and forest condition, with the time-series of annual design-based multivariate panel data, and with multivariate ancillary data from remotely sensed censuses and sample surveys (Czaplewski and others 1988, Czaplewski 1990, 1995, 1999, 2001). This approach does not require stratification of individual FIA panels based on remotely sensed data and geopolitical boundaries, such as counties (Czaplewski 2001). Therefore, the Kalman filter can avoid problems inherent with detailed stratification and when the sample size is small, which is a problem particularly acute with the Moving Average method (Patterson and Reams 2005).

In a sense, the composite estimator in the Kalman filter improves precision by "borrowing" relevant information from the past. Likewise, the Kalman filter can improve precision by "borrowing" ancillary information from remotely sensed sources. Therefore, the Kalman filter is potentially well-suited for complex monitoring systems that include multiple time-series of multivariate remotely sensed data and field data. An example is the Nevada Photo-based Inventory Pilot (NPIP), which is one attempt to implement the national FIA strategic plan (U.S. Forest Service 2007a).

Improving Accuracy of Time-Series Estimates: The mountain pine beetle example in figure 14C and figure 15C used "expert opinion" to quantify model parameters. However, the "extended" Kalman filter (Jazwinski 1970) can simultaneously estimate population attributes and model parameters. Rather than *a priori* expert judgment used to model lodgepole pine damage and mortality as a 50 percent increase per year (figure 14 and figure 15), a potentially more accurate rate parameter could be estimated from the annual panel data, in addition to the estimated mean number of trees per acre. The model form (*e.g*., exponential rate of change) would need to be identified from independent external sources, but the parameter values (*e.g.,* 50 percent per year increase) for the model could be fit empirically without impairing valid inference.

Since forest populations are integrated systems, there can be strong isotropic temporal correlations among variables at proximate points in time, both past and future. More advanced versions of the Kalman filter can act as linear smoothers over multiple time increments (Jazwinski 1970). It is possible that current panel data can improve composite estimates for past conditions in addition to current conditions. This kind of extra effort seems worthwhile when addressing important analysis questions with a relatively short time-series of annual cross-sectional panel data. After all, the cost is over $500,000 for each annual datum point in Colorado.

Multivariate versions of the Kalman filter employ matrix algebra and inverse covariance matrices. Unfortunately, covariance matrices can be ill-conditioned or even singular, especially when the dimensions of the vector estimates are large. These pragmatic circumstances frequently cause numerical instability in large applications of the Kalman filter. In many cases, the numerical results from the Kalman filter will be dominated more by numerical round-off errors than random sampling and prediction errors. This vulnerability can produce disappointing, inaccurate or even infeasible results (e.g., negative variance estimates) with the Kalman filter. Aberrant numerics may not be obvious from the vector estimate alone, which is especially dangerous. Fortunately, variations of the Kalman filter are numerically robust, even with singular covariance matrices (Maybeck 1979). These numerical solutions employ various types of matrix square roots, matrix decompositions or matrix factorizations when combining vector model predictions with design-based vector panel estimates. Bierman (1977) is a particularly useful source for effective solutions to numerical hazards with large, ill-conditioned covariance matrices. While these solutions add complexity during implementation of the Kalman filter, they should not be allowed to distract from the fundamental and intuitive simplicity of the Kalman filter. If there were numerically perfect computers, then the complexity needed to solve numerical problems would not be necessary.

Comparison of FIA Annual and Periodic Surveys for Monitoring

During the 1960s to 1990s, the FIA periodic design produced relatively precise estimates for a “snapshot” in time, but these same estimates often lost much of their value well before the FIA Inventory Unit was re-measured during the following periodic cycle. Users tended to lose confidence in FIA periodic data about 5 years after the field work was completed. Since periodic surveys were repeat only once every 10 to 20 years (AFPA 1998), FIA period surveys had limited value for half or more of their life cycle. How does the current annual FIA design compare with the previous periodic design for monitoring applications?

An annual FIA survey in the Interior West essentially uses the same field plots as the periodic survey. However, those plots are systematically sub-sampled into 10 mutually exclusive FIA panels in the western USA (Bechtold and Patterson 2005). Any single panel includes 1/10th of all FIA field plots. The precision, as measured by the standard deviation of the sample mean, from a single panel equals $(1/\sqrt{10})=0.32$ of the precision from a full periodic survey if both were measured during the exact same time. Therefore, confidence intervals from a single panel are about $(0.32^{-1})=3.1$ times broader than those from a periodic survey conducted in the same year. While there is sufficient funding to measure a single panel in 1 year, there are not enough resources to measure the ten-fold increase in plots every year that would be required for a periodic survey. The annual design sacrifices precision to gain timeliness, although precision remains important in monitoring changes over time.

In order to assess FIA monitoring programs with the current annual design relative to the prior periodic design, hypothetically assume that a periodic FIA survey of Colorado was completed in 2002, with approximately 4,000 forested field plots measured. Therefore, the variance of this hypothetical periodic survey in 2002 would be about 1/10th that of the actual 2002 annual survey. To complete this scenario, visualize annual FIA surveys, each of which measures about 400 forested field plots during a single year, between 2002 and 2007.

Assume that the statewide total number of lodgepole pine trees remains at an approximate steady-state between 2002 and 2007, as described by the model in equations 27 and 28 and used with the Kalman filter for figure 13. Under this model, Figure 16 shows the expected standard deviation of the hypothetical periodic survey in 2002 as an estimate for each year between 2003 and 2007. Figure 16 shows that after 3 years the data quality, as measured by the standard deviation of random estimation errors (σ), of the hypothetical 2002 periodic survey for live trees is approximately the same as the Kalman filter estimate that uses the same model with the much smaller annual surveys from 2002 to 2005. In the absence of new periodic data, and given the stated assumptions, the precision of the Kalman filter estimates for live trees with annual panel data surpasses that of the hypothetical 2002 periodic survey in years 2006 and beyond.

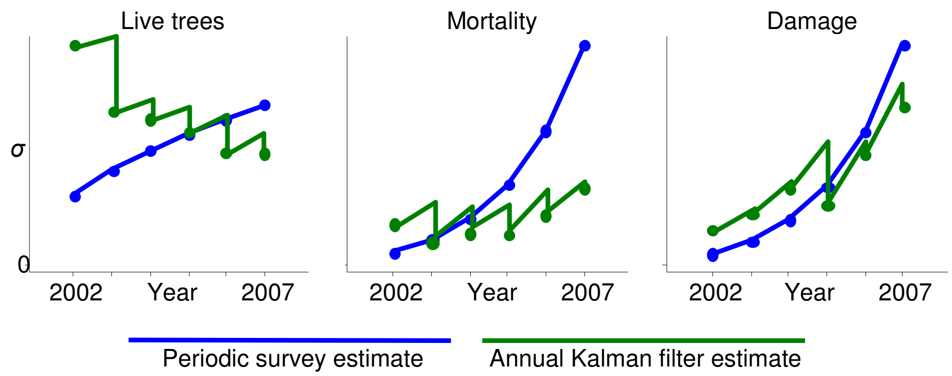

Figure 16: The standard deviation of annual estimates, each with a sample size of *n*/10, compared to that expected from a hypothetical periodic survey in 2002, with a sample size of *n*. A full periodic survey is more accurate (*i.e.,* smaller σ) immediately after all field data are measured, hypothetically in 2002. However, unobserved changes in the population can quickly accumulate after the periodic survey is completed. After 1 to 3 years, the estimated precision of the annual estimates, which are combined with the Kalman filter, equals or surpasses that which would be expected from the corresponding periodic FIA survey, which has 10-times the sample size of a single annual panel. The temporal propagation of error in the design-based periodic survey estimates assumes the same model used for the corresponding annual estimates with the Kalman filter with annual panel data. The model for live lodgepole pine trees assumes a steady-state (figure 13, equations 27 and 28). The models for lodgepole pine tree mortality and damage assumes an exponential increase (figure 14 and figure 15 equations 25 and 26, figure 5). Only the first 5 years after the hypothetical periodic survey are illustrated here. Thereafter, the precision of a periodic survey further deteriorates relative to an annual FIA survey. Likewise, the value of estimates from the periodic survey declines, at least until the next periodic survey. Historically, periodic surveys were conducted once every 10 to 20 years.

As another example, assume that statewide lodgepole pine mortality from mountain pine beetles increases exponentially 50 percent per year between 2002 and 2007. This model is expressed in equations 25 and 26, which is the same model used with the Kalman filter for figure 14C. Assuming this model is approximately true, Figure 16 shows the expected standard deviation of the hypothetical 2002 periodic survey as an estimate of tree mortality for years 2003 through 2007. An example of this same expectation is shown in more detail in figure 5. Almost immediately, the data quality from the annual FIA panels and the Kalman filter exceeds that of the hypothetical periodic survey in 2002, at least under the very dynamic circumstances caused by the mountain pine beetle epidemic in Colorado.

Assuming the same exponential rate of increase in insect damage to live trees, the annual FIA panels with the Kalman filter estimator produces more precise estimates than the hypothetical 2002 periodic survey after only 3 years (figure 16). This hypothetical example demonstrates the potential advantage of the annual FIA design, when coupled with appropriate time-series estimators, for monitoring important changes in a broadly distributed forest population.

Conclusions

The daunting migration by FIA from periodic to annual surveys has improved the timeliness of FIA forest inventory statistics. These have very been useful in strategic analyses of the current state of forests at the national, state and multi-county scales. These results are routinely produced with simple and familiar statistical estimators, namely, the Moving Average or the closely related Temporally Indifferent method. However, a successful monitoring program requires more than production of updated inventory reports (Moffat and others 2008). The Kalman filter not only can improve annual inventory updates when the forest population is undergoing rapid change, the Kalman filter can also improve the ability to monitor, quantify and interpret broad changes in the nation's forests. This is a high priority the FIA strategic plan (U.S. Forest Service 2007a). Hopefully, the descriptions and examples in our paper reveal the benefits and intuitive simplicity of Kalman filter.

The Kalman filter offers other advantages over the Moving Average and Temporally Indifferent methods. The model-based Kalman filter estimator can be more accurate for populations that are rapidly changing, especially if residuals are faithfully monitored to reveal model failures. In populations that are static or change very slowly, it appears that both the Moving Average and Kalman filter estimators yield very similar estimates of current forest inventories.

A properly implemented Kalman filter, which includes analyses of residuals, combines the statistical efficiency of a model-based estimator with the reliability of a design-based estimator. Therefore, the Kalman filter is less vulnerable to temporal "lag bias" (Patterson and Reams 2005) when population dynamics are in a relatively rapid state of flux. This is precisely the situation in which accurate monitoring is most important. This also means that the Kalman filter can be less risky than other model-based estimators when there is a chance that the model is inaccurate.

Unlike the Moving Average and Temporally Indifferent methods, alternative implementations of the Kalman filter can incorporate predictions from alternative deterministic models, which, in turn, are the manifestations of alternative sets of hypotheses. The Akaike information criterion (AIC), which quantifies the agreement between Kalman filter estimates and purely design-based FIA panel estimates, might be used to rank the fit of alternative models to FIA panel data. Therefore, the analyst can quantitatively evaluate alternative *a priori* hypotheses that are intended to explain temporal trends in forest populations. For example, does a model that includes the consequences of climate change better fit the annual FIA design-based panel estimates than a model that assumes no such affects?

The Kalman filter can incorporate deterministic models that consider the population demographics of growth, mortality, regeneration, stand succession, and changes in land use. The Kalman filter can assimilate time-series of diverse remotely sensed data, without the burdensome constraints of post-stratification (Czaplewski 2001). These capabilities can improve precision of inventory and monitoring estimates relative to the Moving Average and Temporally Indifferent methods.

The analyst is initially interested in 3 basic questions: Is there an observable trend in population parameters over time? Does the trend make sense? Is the trend significant relative to the uncertainty in the population estimates? The Kalman filter, much like the Moving Average and Temporally Indifferent methods, can address the first question, at least through the qualitative judgment of the analyst and the temporal series of estimates (see figures 7 through 13).

The time series of estimates from the Moving Average or Temporally Indifferent methods, in concert with the analyst's professional judgment, can address the second question: Does the trend make sense? The Kalman filter is capable of the same. In addition, the Kalman filter, which can objectively rank alternative deterministic models, can progress beyond qualitative judgment, and provide quantitative evidence to answer the second question.

Quantitative evidence is needed to answer the third question: Is the trend significant relative to the uncertainty in the population estimates? The Kalman filter can include a static model in which the population is assumed to be at a steady state, where there the net change over time is zero. The relative fit of this static model compared to alternative dynamic models can be used to make inferences about the third question. The Moving Average and Temporally Indifferent methods do not provide comparable information. Therefore, the Kalman filter improves upon the Moving Average and Temporally Indifferent methods when analyzing temporal trends with FIA annual panel data.

In principle, the Kalman filter offers the opportunity to improve FIA monitoring and analyses. However, this opportunity has not been rigorously tested. Although the fundamental concepts in the Kalman filter are intuitively simple, implementation of the Kalman filter is more complex than current methods used in FIA information management systems. Complexity inescapably incurs risk.

One of the Guiding Principles of the FIA strategic plan (U.S. Forest Service 2007a) is to "*take the lead in inventorying and monitoring changes in the nation's forests, forest resources, and forested ecosystems*." This guidance suggests that additional statistical research by FIA should be directed towards time-series methods that monitor changes in the nation's forests using annual FIA data. The Kalman filter is one such method.

Acknowledgements

Dr. John D. Shaw (U.S. Forest Service, FIA, Ogden, UT) provided the necessary encouragement to further develop the original oral presentation at the 2008 FIA symposium into a full peer-reviewed article in this Proceedings. Drs. Francis A. Roesch (U.S. Forest Service, Asheville, NC), James A. Baldwin (U.S. Forest Service Albany, CA) and KaDonna Randolph (U.S. Forest Service, Knoxville, TN) generously contributed very useful peer reviews. As always, any remaining errors and omissions remain our sole responsibility.

Mr. William Ciesla (U.S. Forest Service, retired, Fort Collins, CO) donated the image of bark beetle damage in figure 11, and Jennifer Ross (U.S. Forest Service, Lakewood, CO) provided the cartographic products used in Figure 12.

Finally, this paper is dedicated to the memory of Dr. Albert R. Stage, who inspired a whole generation of scientists interested in monitoring and forecasting forest conditions in the pursuit of sustainable forestry.

Literature Cited

AFPA. 1998. The report of The Second Blue Ribbon Panel on Forest Inventory and Analysis. Washington, DC: American Forest and Paper Association. 17 p.

Akaike, H. 1974. A new look at the statistical model identification. *Automatic Control, IEEE Transactions on* 19:716-723.

Anderson, D. R. 2008. Model Based Inference in the Life Sciences: A Primer on Evidence. Springer, New York, USA. 184pp.

Bechtold W.A. and P.L. Patterson (editors). 2005 The enhanced forest inventory and analysis program—national sampling design and estimation procedures. Gen. Tech. Rep. SRS-80. Asheville, NC: U.S. Department of Agriculture, Forest Service, Southern Research Station.

Bierman, Gerald J. 1977. Factorization Methods for Discrete Sequential Estimation. Academic Press, NY. 241pp.

Brockwell, P.J.; Davis, R.A. 1996. Introduction to time series and forecasting. New York: Springer Verlag. 420 pp.

Burnham, K. P. and Anderson, D. R. 2001. Kullback-leibler information as a basis for strong inference in ecological studies. *Wildlife Research* 28:111-119.

Burnham, K. P. and Anderson, D. R. 2004. Multimodel inference: Understanding AIC and BIC in model selection. *Sociological Methods & Research* 33:261-304.

Cressie, N. and Wikle, C. K. 2002. Space–time Kalman filter. *In* Encyclopedia of Environmetrics, Volume 4, pp 2045–2049. El-Shaarawi and Piegorsch (Eds.) John Wiley & Sons, Ltd, Chichester

Crookston, N. and Dixon, G. 2005. The forest vegetation simulator: A review of its structure, content, and applications. *Computers and Electronics in Agriculture* 49:60-80.

Crookston, N. L., Rehfeldt, G. E., Ferguson, D. E., and Warwell, M. 2008. FVS and global warming: A prospectus for future development. *In* R. N. Havis and N. L. Crookston (eds.), Third Forest Vegetation Simulator Conference, RMRS-P-54, pp. 7-16. U.S. Department of Agriculture, Forest Service, Rocky Mountain Research Station.

Czaplewski, R. L. 1990. Kalman filter to update forest cover estimates. In V. J. Labau and Cunia (eds.), State-of-the-art methodology of forestry inventory, GTR PNW-263, pp. 457-465. USDA Forest Service, Pacific Northwest Research Station.

Czaplewski, R. L. 1995. Continuous adaptive monitoring of status and trends in ecosystem conditions. Proceedings of the 1995 Society of American Foresters conference. Bethesda, MD: Society of American Foresters. 482 p.

Czaplewski, R. L. 1999. Multistage remote sensing: toward an annual national inventory. *Journal of Forestry*. 97(12):44-48.

Czaplewski, R. 2001 Areal control using generalized least squares as an alternative to stratification , pp. 63-65. In Proceedings of the Second Annual Forest Inventory and Analysis Symposium ; 2000 October 17-18; Salt Lake City, UT. Reams, Gregory A.; McRoberts, Ronald E.; Van Deusen, Paul C., eds. General Technical Report SRS–47. Asheville, NC: U.S. Department of Agriculture, Forest Service, Southern Research Station. 143 p.

Czaplewski, R. L., Alig, R. J., and Cost, N. D. 1988. Monitoring land/forest cover using the Kalman filter: a proposal. *In* Conference on Forest Growth Modelling and Prediction, GTR NC-120, pp. 1089-1096. USDA Forest Service North Central Forest Experiment Station.

Devall, M. S., Grender, J. M., and Koretz, J. 1991. Dendroecological analysis of a longleaf pine *pinus palustris* forest in Mississippi. *Plant Ecology* 93:1-8.

Dixon, B. L., and R. E. Howitt. 1979. Continuous forest inventory using a linear filter. *Forest Science* 25(4):675-689.

Eskelson, B. N. I., Hailemariam, T., and Barrett, T. M. 2008. Tree-level imputation techniques to estimate current plot-level attributes in the pacific northwest using paneled inventory data. *In* W. McWilliams, G. Moisen, and R. Czaplewski (eds.), Forest Inventory and Analysis (FIA) Symposium Proceedings, RMRS-P-56CD, pp. 1-13, Fort Collins, CO. Department of Agriculture, Forest Service, Rocky Mountain Research Station.

Gadbury, G. L.; Williams, M. S.; Schreuder, H. T. 2004. Revisiting the southern pine growth decline: Where are we 10 years later? Gen. Tech. Rep. RMRS-GTR-124. Fort Collins, CO: U.S. Department of Agriculture, Forest Service, Rocky Mountain Research Station. 10 p..

Gartner, D. and Reams, G. 2002. A comparison of several techniques for imputing tree level data. *In* R. E. Mcroberts, G. A. Reams, P. C. Van Deusen, and J. W. Moser (eds.), Proceedings of the Third Annual Forest Inventory and Analysis Symposium, General Technical Report GTR-NC-230, pp. 103-108. U.S. Department of Agriculture, Forest Service, North Central Research Station.

Gao, C., Wang, H., Lakshmivarahan, S., Weng, E., Zhang, Y., and Luo, Y. 2008. Parameter estimation and uncertainty analysis of forest carbon dynamics: Ensemble Kalman filter method. *In* 93rd Annual Meeting of the Ecological Society of America: Enhancing Ecological Thought by Linking Research and Education.

Goodwin, N. R., 2008. Estimation of insect infestation dynamics using a temporal sequence of landsat data. *Remote Sensing of Environment* 112:3680-3689.

Gove, J. and Houston, D. 1996. Monitoring the growth of american beech affected by beech bark disease in Maine using the Kalman filter. *Environmental and Ecological Statistics* 3:167-187.

Gregoire, T. G. and D.K. Walters. 1988. Composite vector estimator by weighting inversely proportional to variance, *Canadian Journal of Forest Research*. 18:282–284.

Hurteau, M., H. Zald, and M. North 2007. Species-specific response to climate reconstruction in upper-elevation mixed-conifer forests of the western Sierra Nevada, California. *Canadian Journal of Forest Research* 37:1681-1691.

Jazwinski, A. H. 1970. Stochastic Processes and Filtering Theory. Academic Press, NY. 376pp

Johnson, D.S.; Williams, M.S.; Czaplewski, R.L. 2003. Comparison of estimators for rolling samples using forest inventory and analysis data. *Forest Science*. 49(1): 50-63.

Johnson, E. W.; and D. Wittwer. 2006. Aerial detection surveys in the United States *In*: Aguirre-Bravo, C.; Pellicane, Patrick J.; Burns, Denver P.; and Draggan, Sidney, Eds. 2006. Monitoring Science and Technology Symposium: Unifying Knowledge for Sustainability in the Western Hemisphere Proceedings RMRS-P-42CD. Fort Collins, CO: U.S. Department of Agriculture, Forest Service, Rocky Mountain Research Station. pp. 809-811.

Kish, L. 1987. Statistical Design for Research. John Wiley & Sons.

Kott, P. 2005. Randomization-assisted model-based survey sampling. *Journal of Statistical Planning and Inference* 129:263-277.

Lessard, V. C., McRoberts, R. E., and Holdaway, M. R. 2001. Diameter growth models using Minnesota Forest Inventory And Analysis data. *Forest Science* 47:301-310.

Logan, J. A., Régnière, Â., and Powell, Â. A. 2003. Assessing the impacts of global warming on forest pest dynamics. *Frontiers in Ecology and the Environment* 1:130-137.

Malmstrom, C. M. and Raffa, K. F. 2000. Biotic disturbance agents in the boreal forest: considerations for vegetation change models. *Global Change Biology* 6:35-48.

Maybeck, P. S. 1979. Stochastic models, estimation, and control. Volume 1. Academic Press, NY. 423pp.

McRoberts R.E. 2001. Imputation and model-based updating techniques for annual forest inventories. Forest Science 47:322-330.

McRoberts, R. E. 2005. The enhanced forest inventory and analysis program. Gen. Tech. Rep. SRS-80. Asheville, NC: U.S. Department of Agriculture, Forest Service, Southern Research Station. 1-10

Meinhold, J. and Singpurwalla, N.D. 1983. Understanding the Kalman filter. *The American Statistician* 37:123–127.

Miles, P. D. 2008. Forest inventory and analysis data for FVS modelers. In: Havis, Robert N.; Crookston, Nicholas L., comps. 2008. Third Forest Vegetation Simulator Conference; 2007 February 13Â–15; Fort Collins, CO. Proceedings RMRS-P-54. Fort Collins, CO: U.S. Department of Agriculture, Forest Service, Rocky Mountain Research Station. p. 125-129

Moffat, A. J., Davies, S., and Finr, L. 2008. Reporting the results of forest monitoring: an evaluation of the European forest monitoring programme. *Forestry* 81:75-90.

Ni, C. and Zhang, L. 2008. An estimator of prediction error variance for projection equations. *Forest Science* 54:569-578.

Patterson, P. L; and G. A. Reams. 2005. Combining panels for forest inventory and analysis estimation. pp. 69-74 *In*: W.A. Bechtold and P.L. Patterson, eds. The enhanced forest inventory and analysis program—national sampling design and estimation procedures. Gen. Tech. Rep. SRS-80. Asheville, NC: U.S. Department of Agriculture, Forest Service, Southern Research Station.

Pollard, J. E.; J. A. Westfall, P. L. Patterson, D. L Gartner, M. Hansen, O. Kuegler. 2006. Forest Inventory and Analysis National Data Quality Assessment Report for 2000 to 2003 Gen. Tech. Rep. RMRS-GTR-181. Fort Collins, CO: U.S. Department of Agriculture, Forest Service, Rocky Mountain Research Station. 43 pp.

Reams, G. A. and McCollum, J. M. 2000. The use of multiple imputation in the southern annual forest inventory system. *In* M. Hansen and T. Burk (eds.), Integrated tools for natural resources inventories in the 21st century., General Technical Report GTR-NC-212, pp. 228-233.

Reams, G. A.; W. D Smith; M. H. Hansen; W. A. Bechtold; F. A. Roesch; and G. G. Moisen. 2005. pp. 21-36 *In*: W.A. Bechtold and P.L. Patterson, eds. The enhanced forest inventory and analysis program—national sampling design and estimation procedures. Gen. Tech. Rep. SRS-80. Asheville, NC: U.S. Department of Agriculture, Forest Service, Southern Research Station.

Roesch, F. A. 1999. Mixed estimation for a forest survey sample design, pp. 1-6. In 1999 Proceedings of the Section on Statistics and the Environment, American Statistical Association, Presented at the Joint Statistical Meetings Baltimore, MD August 8-12, 1999. 148 p.

Roesch, F. A. 2007. Compatible estimators of the components of change for a rotating panel forest inventory design. *Forest Science* 53(1):50-61.

Roesch. F. A. 2008 Spatial-Temporal Models for Improved County-Level Annual Estimates. *In*: McWilliams, Will; Moisen, Gretchen; Czaplewski, Raymond, comps. 2008. Forest Inventory and Analysis (FIA) Symposium 2008; October 21-23, 2008; Park City, UT. Proc. RMRS-P-56CD, pp. 1-20. Fort Collins, CO: U.S. Department of Agriculture, Forest Service, Rocky Mountain Research Station. 1 CD.

Roesch, F.A. and G.A. Reams, 1999. Analytical alternatives for an annual inventory system. *Journal of Forestry*. 97: 33-37.

Särndal, C., B. Swensson, and J. Wretman. 1992. Model Assisted Survey Sampling. Springer, New York. 694pp.

Schwarz, G. 1978. Estimating the dimension of a model. *Annals of Statistics* 6:461-464.

Scott, C.T. and M. Köhl. 1993. Experiences with designing the Forest Survey of the Northeastern U.S. Proc. Statistical Methods, Mathematics and Computers. Köhl, M. and G.Z. Gertner, ed., Berlin/Eberswalde, Germany. Swiss Federal Institute for Forest, Snow and Landscape Research, Birmensdorf, Switzerland. pp. 139-148

Scott, C. T.; W. A. Bechtold; G. A. Reams; W. D. Smith; J. A. Westfall; M. H. Hansen; and G. G Moisen. 2005. Sample-based estimators used by the forest inventory and analysis national information management system. pp. 43-67 *In*: W.A. Bechtold and P.L. Patterson, eds. The enhanced forest inventory and analysis program—national sampling design and estimation procedures. Gen. Tech. Rep. SRS-80. Asheville, NC: U.S. Department of Agriculture, Forest Service, Southern Research Station.

Theil, H. 1971. Principles of econometrics. Wiley, New York

Tian, X. and Xie, Z. 2008. A land surface soil moisture data assimilation framework in consideration of the model subgrid-scale heterogeneity and soil water thawing and freezing. S*cience in China Series D: Earth Sciences* 51:992-1000.

U.S. Forest Service . 2007a. Forest Inventory and Analysis Strategic Plan: A History of Success, a Dynamic Future. FS-865. Washington, DC: U.S. Forest Service . 17 pp.

U.S. Forest Service . 2007b. Interior West Forest Inventory and Analysis Field Procedures, Version 3.01. Ogden, UT: U.S. Forest Service , Rocky Mountain Research Station.

Van Den Brakel, J. A. and Visser, H. 1996. The influence of environmental conditions on tree-ring series of Norway spruce for different canopy and vitality classes. *Forest Science* 42:206-219.

Van Deusen, P. C. 1987. Testing for stand dynamics effects on red spruce growth trends. *Canadian Journal of Forest Research* 17:1487-1495

Van Deusen, P. C. 1989. A model-based approach to tree ring analysis. *Biometrics* 45:763-779.

Van Deusen, P. C. 1997. Annual forest inventory statistical concepts with emphasis on multiple imputation. *Can. J. For. Res.* 27:379-384.

Van Deusen, P. C. 1999. Modeling trends with annual survey data. *Canadian Journal of Forest Research* 29:1824-1828.

Van Deusen, P.C. 2002. Comparison of some annual forest inventory estimators. *Canadian Journal of Forest Research*. 32: 1992-1995.

Van Deusen, P.C. 2008. Detecting trend in annual inventory data with a mixed estimator. *In*: McWilliams, Will; Moisen, Gretchen; Czaplewski, Raymond, comps. 2008. Forest Inventory and Analysis (FIA) Symposium 2008; October 21-23, 2008; Park City, UT. Proc. RMRS-P-56CD. Fort Collins, CO: U.S. Department of Agriculture, Forest Service, Rocky Mountain Research Station. 1 CD.

Visser, H. and Molenaar, J. 1992. Estimating trends and stochastic response functions in dendroecology with an application to fir decline. *Forest Science* pp. 221-234.

Walters, D. K., Burkhart, H. E., Reynolds, M. R., and Gregoire, T. G. 1991. A Kalman filter approach to localizing height-age equations. *Forest Science* pp. 1526-1537.

Williams, M., Schwarz, P. A., Law, B. E., Irvine, J., and Kurpius, M. R. An improved analysis of forest carbon dynamics using data assimilation. *Global Change Biology* 11:89-105

Wulder, M., Dymond, C., White, J., Leckie, D., Carroll, A. 2005. Surveying mountain pine beetle damage of forests: A review of remote sensing opportunities. *Forest Ecology and Management* 221(1–3):27-41.

Wulder, M. A., White, J. C., Bentz, B. J., Alvarez, M. F., and Coops, N. C. 2006a. Estimating the probability of mountain pine beetle red-attack damage. *Remote Sensing of Environment* 101:150-166.

Wulder, M. A., White, J. C., Bentz, B. J., and Ebata, T. 2006b. Augmenting the existing survey hierarchy for mountain pine beetle red-attack damage with satellite remotely sensed data. *Forestry Chronicle* 82:187-202.